

 Open access • Posted Content • DOI:10.1101/813592

A microtranslatome coordinately regulates sodium and potassium currents in the heart

— [Source link](#) 

Catherine A. Eichel, Erick B. Ríos-Pérez, Fang Liu, Margaret B. Jameson ...+4 more authors

Institutions: University of Wisconsin-Madison, University of Michigan

Published on: 21 Oct 2019 - bioRxiv (Cold Spring Harbor Laboratory)

Topics: hERG

Related papers:

- [A microtranslatome coordinately regulates sodium and potassium currents in the human heart.](#)
- [Cotranslational association of mRNA encoding subunits of heteromeric ion channels.](#)
- [RNA interference reveals that endogenous *Xenopus* MinK-related peptides govern mammalian K⁺ channel function in oocyte expression studies.](#)
- [Cyclic AMP regulates the HERG K\(+\) channel by dual pathways.](#)
- [Alternative splicing determines mRNA translation initiation and function of human K2P10.1 K⁺ channels](#)

Share this paper:    

View more about this paper here: <https://typeset.io/papers/a-microtranslatome-coordinately-regulates-sodium-and-lo1zpbkg0t>

1 **A microtranslatome coordinately regulates sodium and potassium currents in**
2 **the heart**

3

4

5 Catherine A. Eichel¹, Erick B. Ríos-Pérez¹, Fang Liu¹, Margaret B. Jameson¹, David
6 K. Jones^{1,2}, Jennifer J. Knickelbine¹ and Gail A. Robertson^{1*}

7

8

9 ¹Dept. of Neuroscience and Cardiovascular Research Center
10 University of Wisconsin School of Medicine and Public Health
11 1111 Highland Ave. #5505
12 Madison, WI 53705

13

14 ²Current address: Dept. of Pharmacology
15 University of Michigan Medical School
16 Ann Arbor, MI 48109

17

18 *Corresponding author: garobert@wisc.edu

19

20

21

22

23

24

25 **Keywords:** action potential, ion channels, co-knockdown, arrhythmia, KCNH2, Kv11.1,
26 Na_v1.5, cotranslational

27

28

29

30

31 **ABBREVIATION LIST**

32 AP: Action potential

33 APD: Action potential duration

34 Co-IP: Co-immunoprecipitation

35 ER: Endoplasmic reticulum

36 FISH: Fluorescence in-situ hybridization

37 IF: Immunofluorescence

38 IP: Immunoprecipitation

39 iPSC-CM: Cardiomyocyte derived from induced pluripotent stem cells

40 RBP: RNA binding protein

41 RNA-IP: RNA-immunoprecipitation

42 shRNA: Short hairpin RNA

43

44

45

46

47 **ABSTRACT**

48

49 Catastrophic arrhythmias and sudden cardiac death can occur with even a small imbalance
50 between inward sodium currents and outward potassium currents, but mechanisms
51 establishing this critical balance are not understood. Here, we show that mRNA transcripts
52 encoding I_{Na} and I_{Kr} channels (*SCN5A* and *hERG*, respectively) are associated in defined
53 complexes during protein translation. Using biochemical, electrophysiological and single-
54 molecule fluorescence localization approaches, we find that roughly half the *hERG*
55 translational complexes contain *SCN5A* transcripts. Moreover, the transcripts are regulated
56 in a way that alters functional expression of both channels at the membrane. Association and
57 coordinate regulation of transcripts in discrete “microtranslatomes” represents a new
58 paradigm controlling electrical activity in heart and other excitable tissues.

59

60

61

62

63

64

65 **INTRODUCTION**

66

67 Signaling in excitable cells depends on the coordinated flow of inward and outward currents
68 through a defined ensemble of ion channel species. This is especially true in heart, where
69 the expression of many different ion channels controls the spread of excitation triggering the
70 concerted contraction of the ventricular myocardium. Even small perturbations in the
71 quantitative balance due to block or mutations affecting a single type of channel can initiate
72 or perpetuate arrhythmias and lead to sudden death. Repolarization is a particularly
73 vulnerable phase of the cardiac cycle, when imbalance of inward and outward currents can
74 prolong action potential duration and trigger arrhythmias such as Torsades de Pointes¹. The
75 genetic basis of such catastrophic arrhythmias is in many cases unknown; mechanisms
76 coordinating expression of multiple ion channels may represent novel disease targets.

77

78 Cardiac I_{Kr} is critical for normal repolarization² and is a major target of acquired and
79 congenital long QT syndrome^{3,4}. I_{Kr} channels minimally comprise hERG1a and hERG1b
80 subunits^{5,6}, which associate cotranslationally⁷ and preferentially form heteromultimers⁸.
81 Underlying heteromultimerization is the cotranslational association of *hERG1a* and *1b* mRNA
82 transcripts⁹. Because current magnitude is greater in heteromeric hERG1a/1b vs. homomeric
83 hERG1a channels, and loss of hERG1b is pro-arrhythmic^{5,10}, the mechanism of
84 cotranslational assembly of hERG subunits is important in cardiac repolarization⁹.

85

86 In this study we found that association of transcripts could occur not only between alternate
87 *hERG* transcripts encoded by a single gene locus, but also between transcripts encoding
88 entirely different ion channel types whose balance is critical to cardiac excitability. Indeed, we
89 show that *SCN5A*, encoding the cardiac Na_v1.5 sodium channel, associates with *hERG*
90 transcripts as demonstrated by co-immunoprecipitation of nascent protein in heterologous
91 expression systems, cardiomyocytes derived from human induced pluripotent stem cells, and
92 native human myocardium. Single-molecule fluorescent *in situ* hybridization (smFISH)

93 quantitatively reveals *hERG* and *SCN5A* transcript colocalization captured during protein
94 translation. Targeting *hERG* transcripts for shRNA degradation coordinately reduces *SCN5A*
95 transcript levels as well, along with native I_{Kr} and I_{Na} currents recorded from cardiomyocytes.
96 Thus, cotranslational association and regulation of transcripts is a novel mechanism
97 establishing and preserving a balance of I_{Kr} and I_{Na} in heart, where relative levels of these
98 currents are critical for normal action potential production and coordinated electrical activity.

99
100
101
102
103
104
105

106 **RESULTS**

107 **Copurification of *hERG 1a* and *SCN5A* transcripts with their encoded proteins**

108 Using specific antibodies that target the N-terminus of hERG1a, we purified hERG1a protein
109 from induced pluripotent stem cell-derived cardiomyocytes (iPSC-CMs) and human ventricle
110 lysates and performed RT-PCR to identify associated transcripts (“RNA-IP”; Fig. 1a). As
111 previously reported⁹, both *hERG1a* and *1b* transcripts co-immunoprecipitated with nascent
112 hERG 1a protein. Surprisingly, *SCN5A* transcripts encoding Na_v1.5 channels also copurified
113 with nascent hERG1a protein (Fig. 1b and Supplementary Fig. S1). The interaction appears
114 specific since neither ryanodine receptor RyR2 nor inward rectifier channel Kir2.1 (*KCNJ2*)
115 transcripts copurified as part of this complex. The counterpart experiment using anti-Na_v1.5
116 antibodies confirmed association of transcripts encoding hERG1a, hERG1b and Na_v1.5, but
117 not RyR2 (Fig. 1b). Bead-only controls showed no signal, indicating specific interactions of
118 antibodies with corresponding antigens. The association also occurred in HEK293 cells,
119 where additional controls showed that the antibodies used did not interact nonspecifically
120 with mRNA encoding the other ion channels or subunits (Supplementary Fig. S1).
121 Interestingly, when lysates independently expressing hERG1a and Na_v1.5 were mixed,
122 hERG1a antibodies copurified only *hERG1a* mRNA, and Nav1.5 antibodies copurified only
123 *SCN5A* mRNA, indicating that association of the two mRNAs requires their co-expression *in*
124 *situ*. In addition, the interaction between *hERG1a* and *SCN5A* does not require the presence
125 of *hERG1b* (Supplementary Fig. S1). This experiment demonstrates that transcripts
126 encoding hERG1a, hERG1b and Na_v1.5 physically interact within the cell and can be
127 copurified using antibodies targeting either nascent hERG1a or Na_v1.5 proteins. Their
128 association with either encoded protein implies the transcripts associate during protein
129 translation, or *cotranslationally*.

130

131 ***hERG1a* and *SCN5A* transcript distribution**

132 To independently confirm *hERG1a* and *SCN5A* transcript association, we performed single-
133 molecule fluorescence *in situ* hybridization (smFISH) experiments in iPSC-CMs (Fig. 2a). We

134 used a combination of short DNA oligonucleotides (20 nucleotides), each labelled with a
135 single fluorophore, that bind in series on the target mRNA and collectively are detected as a
136 single fluorescent spot¹¹ (see Methods). Probes for *hERG1a* and *SCN5A* mRNAs were
137 designed with spectrally separable labels for simultaneous detection (Quasar 647 and 546
138 respectively; see Methods and Supplementary Fig. S2 for probe validation, and Table S1 for
139 list of probes)¹². Punctate signal for each mRNA species appeared singly and in clusters (Fig.
140 1a, b). To evaluate mRNA copy number in each detected signal, we fitted the histogram of
141 the total fluorescence intensity of smFISH signals with the sum of Gaussian functions and
142 determined mean intensity of a single mRNA molecule for each species (Fig. 2b and
143 Supplementary Fig. S3). We found that approximately 25% of detected molecules exist
144 singly, whereas about 20% occupy clusters containing 6 or more transcripts (Fig. 2c). Both
145 transcripts were observed throughout the cytoplasm with higher density within 5-10 μm from
146 the nucleus (Fig. 2a, d), consistent with the expected distribution of perinuclear endoplasmic
147 reticulum where these mRNA molecules are translated into proteins. A *GAPDH* mRNA probe
148 set served as a positive control for smFISH experiments (Stellaris[®] validated control). In
149 contrast with signals observed for *hERG1a* and *SCN5A* transcripts, *GAPDH* transcript
150 clustered less, with 50% found as single molecules and <5% in clusters of 6 or more
151 transcripts (Fig. 2c). Moreover, *GAPDH* molecules distributed more homogeneously
152 throughout the cytoplasm with higher density in the range of 10 to 20 μm from the nucleus
153 (Fig. 2d). We noted similar numbers of *hERG1a* and *SCN5A* transcripts per cell but fewer
154 than those for *GAPDH* (Fig. 2e). Thus, numbers and spatial distribution of *hERG1a* and
155 *SCN5A* transcripts can be simultaneously resolved. Further work will be required to elucidate
156 the significance or possible physiological role of differently sized mRNA clusters.

157

158 ***hERG1a* and *SCN5A* transcript expression levels correlate**

159 Although we observed a range in numbers of *hERG1a* and *SCN5A* mRNAs among iPSC-
160 CMs (Fig. 2e), regression analysis revealed clear correlation in their expression levels within

161 a given cell (Fig. 3 and Supplementary Table S3). Plotted against each other, *hERG1a* and
162 *SCN5A* mRNA numbers exhibited a coefficient of determination (R^2) of 0.57 ($P=0.00001$; 41
163 cells; Fig. 3a and b). In contrast, pairwise combinations of *hERG1a* and *RyR2*, *hERG1a* and
164 *GAPDH*, or *SCN5A* and *GAPDH* exhibited much lower linear correlation ($R^2=0.22$, $P=0.017$;
165 $R^2=0.18$, $P=0.15$; and $R^2=0.33$, $P=0.000134$ respectively; $n=26$, 13, and 28 cells respectively;
166 Fig. 3c and d, Supplementary Fig. S5 a and b, and Supplementary Table S3). Spearman
167 coefficients revealed similar results as Pearson coefficients, where significant correlation is
168 observed only between *SCN5A* and *hERG1a* (Supplementary Table S3). These findings
169 indicate a roughly constant ratio of *hERG1a* and *SCN5A* mRNA copies.

170

171 ***hERG1a* and *SCN5A* transcripts colocalize**

172 To determine potential *hERG1a* and *SCN5A* transcript association using smFISH, we
173 measured proximity between the two signals using the centroid position, scored from
174 touching to 67% (1 pixel) overlap (Fig. 4a and b). To discern colocalization from random
175 overlap, we calculated the expected number of particles that could associate based on
176 chance only for the different association criteria. Two-tailed *t* tests with Bonferroni correction
177 revealed association between *hERG1a* and *SCN5A* transcripts significantly greater than that
178 expected by chance (see Methods; *P* values summarized in Supplementary Table S2; Fig.
179 4b). Approximately 25% of each transcript population was associated with the other (Fig. 4c).
180 To test specificity of interaction between *hERG1a* and *SCN5A* transcripts, smFISH and
181 pairwise comparisons were also performed with *RyR2* and *GAPDH* transcripts, which
182 revealed no significant association (Fig. 4d and e; Supplementary Table S2). These results
183 show that association of *hERG* and *SCN5A* transcripts demonstrated in lysates can also be
184 visualized in iPSC-CMs *in situ*, and provide strong evidence for the existence of a discrete
185 mRNA complex comprising *hERG1a* and *SCN5A* transcripts.

186

187

188

189 **Discrete *hERG1a* and *SCN5A* cotranslational complexes**

190 To further explore whether colocalized mRNAs were part of a translational complex, we
191 combined smFISH with immunofluorescence using hERG1a antibodies. We observed close
192 association between *hERG1a* and *SCN5A* mRNAs and hERG1a protein significantly greater
193 than that expected by chance (Fig. 5a and b and Supplementary Fig. S6a and b).

194 Interestingly, among the 16% of actively translated *hERG1a* mRNAs (i.e. those associated
195 with hERG1a protein), 46% were also associated with *SCN5A* mRNAs (Fig. 5c), indicating a
196 3-fold enrichment of their association in translational complexes. Analysis of the distribution
197 of colocalized molecules revealed that 70% are located close to the nucleus (within 10 μ m,
198 Fig. 5d).

199

200 We monitored association of hERG1a protein and transcript in the presence of puromycin,
201 which releases translating ribosomes from mRNAs¹³ (Fig. 6a). We observed no change due
202 to puromycin in the total number of respective mRNAs detected per cell (Fig. 6b). As
203 expected, puromycin reduced association between *hERG1a* mRNA and hERG1a protein
204 (antibody) and the S6 ribosomal protein (Fig. 6c). In addition, triple colocalization of *hERG1a*
205 and *SCN5A* transcripts and either hERG1a protein or the ribosomal subunit S6 was robustly
206 reduced (Fig 6d). These findings further support the conclusion that *hERG1a* and *SCN5A*
207 associate cotranslationally.

208

209 ***hERG1a* and *SCN5A* mRNAs are coregulated**

210 We previously demonstrated that targeted knockdown of either *hERG1a* or *1b* transcripts by
211 specific short hairpin RNA (shRNA) caused a reduction of both transcripts not attributable to
212 off-target effects in iPSC-CMs or in HEK293 cells⁹. To determine whether *hERG* and *SCN5A*
213 transcripts are similarly subject to this co-knockdown effect, we evaluated expression levels
214 by performing RT-qPCR experiments in iPSC-CM. We found that *hERG1a*, *hERG1b* and
215 *SCN5A* expression levels were all reduced by about 50% upon *hERG1a* silencing compared
216 to the effects of a scrambled shRNA (Fig. 7a, orange bars). *RYR2* transcript levels were

217 unaffected. We observed similar results using the specific *hERG1b* shRNA (Fig. 7a, blue
218 bars). Expressed independently in HEK293 cells, only *hERG1a* mRNA was affected by the
219 1a shRNA, and only *hERG1b* was affected by the 1b shRNA (Fig. 7b). *SCN5A* was
220 unaffected by either shRNA, indicating that the knockdown in iPSC-CMs was not due to off-
221 target effects and levels of associated *hERG1a* and *SCN5A* are quantitatively coregulated.
222 Similar results of approximately 40% co-knockdown of discrete *hERG1a* and *SCN5A* mRNA
223 particles were obtained using smFISH (Supplementary Fig. S7). Even more than the total
224 population of mRNA, the number of colocalized particles is decreased by approximately
225 55%, indicating that physically associated transcripts are subjected to co-knockdown (Fig.
226 S7c). Together these results indicate a coordinated and quantitative regulation of mRNAs
227 encoding a complement of ion channels.

228

229 ***I_{Kr}* and *I_{Na}* are coregulated**

230 To assess functional consequences of transcript coregulation, we recorded effects of
231 *hERG1b* silencing on native currents in iPSC-CMs. Fig. 7c shows the repolarizing current *I_{Kr}*
232 in iPSC-CMs transfected with either *hERG1b* or scrambled shRNA. Steady state and peak
233 tail *I_{Kr}* were decreased in *hERG1b*-silenced cells compared to cells transfected with
234 scrambled shRNA (Fig. 7d). *I_{Kr}* reduction was the result of a decrease in G_{\max} upon *hERG1b*-
235 specific silencing with no modifications in the voltage dependence of activation (Fig. 7e and
236 Supplementary Table S4). These results are in accordance to our previous studies reporting
237 a reduction in *I_{Kr}* density upon *hERG1b*-specific silencing, and indicate that transcripts
238 targeted by shRNA are those undergoing translation^{9,10}. To determine whether *hERG1b*
239 silencing also affects translationally active *SCN5A*, we measured peak *I_{Na}* density in iPSC-
240 CMs and detected significant reduction of about 60% when *hERG1b* was silenced, compared
241 to control cells (Fig. 7f, g and h). Peak G_{\max} was decreased but no alterations in voltage
242 dependence of activation or inactivation were detected (Fig. 7h and Supplementary Tables
243 S4 and S5). Late *I_{Na}*, measured as the current integral from 50 to 800 ms from the beginning
244 of the pulse¹⁴, was similarly reduced in magnitude (Fig. 7i, j and k). This analysis indicates

245 that coregulation via co-knockdown results in quantitatively similar alteration of $I_{Na,late}$ and I_{Kr} ,
246 which operate together to regulate repolarization¹⁵. I_{to} , which does not regulate action
247 potential duration in larger mammals¹⁶, is unaffected by *hERG1b* silencing (Fig. 8a, b, c and
248 d), suggesting the coregulation of I_{Na} and I_{Kr} reflects their coherent participation in
249 repolarization.
250
251
252

253 DISCUSSION

254 We have demonstrated using diverse and independent approaches the association and
255 coregulation of transcripts encoding ion channels that regulate excitability in cardiomyocytes.
256 By co-immunoprecipitating mRNA transcripts along with their nascent proteins, we have
257 shown that *hERG* and *SCN5A* transcripts associate natively in human ventricular
258 myocardium and iPSC-CMs as well as when heterologously expressed in HEK293 cells.
259 Using smFISH together with immunofluorescence in iPSC-CMs, we demonstrate that the
260 ratio of *hERG* and *SCN5A* transcripts is approximately 1:1 despite a range of pool sizes from
261 roughly 5 to 200 molecules per cell. These transcripts colocalize about 25% of the time, but
262 when considering only those *hERG* transcripts undergoing translation, nearly 50% are
263 associated with *SCN5A*. When *hERG1a* or *hERG1b* transcripts are targeted by shRNA,
264 *SCN5A* levels are reduced by about the same amount. Both peak and late I_{Na} are
265 correspondingly reduced. Reflecting their coherent roles in the process of cardiac
266 repolarization, the term “microtranslatome” captures the cotranslational properties of this
267 discrete complex comprising functionally related mRNAs and their nascent proteins.
268
269 What is the functional role of cotranslational association of transcripts? Deutsch and
270 colleagues showed that cotranslational interaction of nascent Kv1.3 N-termini facilitates
271 proper tertiary and quaternary structure required for oligomerization^{17,18}. Cotranslational
272 heteromeric association of hERG1a and hERG1b subunits ensures cardiac I_{Kr} has the
273 appropriate biophysical properties and magnitude shaping the normal ventricular action
274 potential. Coordinated protein translation of *different* channel types could control relative
275 numbers of ion channels involved in electrical signaling events. Such a balance is critical
276 during repolarization, when alterations in I_{Kr} or late I_{Na} are known to cause arrhythmias
277 associated with long QT syndrome or Brugada syndrome¹⁹⁻²¹. Indeed, during normal Phase 3
278 repolarization, non-equilibrium gating of sodium channels leads to recovery from inactivation
279 and re-activation of currents substantially larger than the tiny steady-state late I_{Na} observed
280 under voltage-clamp steps^{15,22}. Our observation of roughly equivalent *hERG1a* and *SCN5A*

281 mRNA levels squares with previous reports of fixed channel transcript ratios associated with
282 certain identified crustacean neurons^{23,24}. Cotranslating mRNAs in a stoichiometric manner
283 could buffer noise associated with transcription²⁵ and render a stable balance of channel
284 protein underlying control of membrane potential.

285

286 These studies raise questions of the mechanism by which transcripts associate. Although
287 hERG1a and hERG1b N-termini interact during translation⁷, association of transcripts does
288 not rely on this interaction: alternate transcripts encoding the proteins interact even when
289 translation of one of the proteins is prevented⁹. In principle, transcripts could associate via
290 complementary base pairing or by tertiary structural interactions as ligand and receptor.
291 Alternatively, they could be linked by one or more RNA binding proteins (RBPs). Because the
292 association and coregulation observed in native heart can be reproduced in HEK293 cells,
293 the same or similar mechanisms are at work in the two systems. More work will be required
294 to discern among possible mechanisms, and to determine the time course with respect to
295 transcription, nuclear export and cytosolic localization of interacting transcripts.

296

297 A mechanism involving RBPs is appealing because it comports with the idea of the “RNA
298 regulon,” a term describing a complex of transcripts bound by one or more RBPs^{26,27}. RBPs
299 in the yeast Puf family bind large collections of mRNAs to control their localization, stability,
300 translation and decay^{28,29}. In mammalian systems, the Nova protein serves to coordinate
301 expression of mRNAs encoding splicing proteins important in synaptic function³⁰.

302 Presumably in both cases these proteins interact in multiple regulons (complexes) serving
303 different or related roles. Mata and colleagues isolated individual mRNA species in yeast and
304 showed they associate with other mRNAs encoding functionally related (but nonhomologous)
305 proteins, along with mRNA encoding the RBP itself³¹. Moreover, these mRNAs encoded
306 proteins that formed stable macromolecular complexes³². Taking it one step further, Cosker
307 et al. showed that two mRNAs involved in cytoskeletal regulation bind the same RBP to form

308 a single RNA granule³³, possibly analogous to the microtranslatome regulating key elements
309 of excitability in the heart reported here.

310

311 A comprehensive analysis of the microtranslatome's components will require RNA-seq at a
312 level of multiplexing that ensures sufficient statistical power in the face of potentially reduced
313 complexity of the RNA-IP samples. These efforts will necessarily be followed by validation
314 through complementary approaches such as RNAi and smFISH to confirm their identity
315 within the microtranslatome.

316

317 One of the more curious findings of our study is the coordinate knockdown of different
318 mRNAs in the complex by shRNAs targeted to only one of the mRNA species. The
319 mechanism by which multiple mRNA species may be simultaneously regulated is not clear.
320 shRNAs silence gene expression by producing an antisense (guide) strand that directs the
321 RNA-induced silencing complex (RISC) to cleave, or suppress translation of, the target
322 mRNA^{34,35}. Since hERG shRNA has no off-target effect on *SCN5A* mRNA expressed
323 heterologously in HEK293 cells, we assume there is insufficient complementarity for a direct
324 action. Perhaps by proximity to RISC, translation of the nontargeted mRNA is also disrupted,
325 but to our knowledge no current evidence is available to support this idea. A transcriptional
326 feedback mechanism seems unlikely given that co-knockdown can occur with plasmids
327 transiently expressed from engineered promoters and not integrated into the genome of
328 HEK293 cells. It is also important to note that it is unknown whether *SCN5A* is the only
329 sodium channel transcript coregulated by *hERG* knockdown. In principle, transcripts
330 encoding other sodium channels implicated in late I_{Na} , such as Nav1.8^{36,37}, could also be
331 affected, as could transcripts encoding auxiliary subunits associated with Nav1.5³⁸.

332

333 Whether disrupting the integrity of these complexes gives rise to some of the many
334 arrhythmias not attributable to mutations in ion channel genes *per se* remains to be
335 determined. Although the coregulation of inward I_{Na} and outward I_{Kr} shown in this study may

336 suggest a compensatory mechanism, in a previous study we showed that selective
337 knockdown of *hERG1b* prolongs action potential duration and enhances variability, both
338 cellular markers of proarrhythmia¹⁰. Perhaps in the absence of co-regulation the effects
339 would be more deleterious. Jalife and colleagues have introduced the concept of the
340 “channelosome,” a macromolecular protein complex mediating a physiological action.
341 Interestingly, Nav1.5 and Kir2.1, which regulates resting and diastolic membrane potential,
342 exhibit compensatory changes when the levels of either are genetically manipulated³⁹. In this
343 case, the effect seems to be on stability of the nontargeted channel proteins, which form a
344 complex together with SAP97, and not on mRNA levels⁴⁰. We do not yet know whether the
345 complex of transcripts we have studied encodes a similarly stable macromolecular complex,
346 or perhaps ensures appropriate ratios of channels distributed independently at the
347 membrane. Based on current evidence, we propose that the microtranslatome of associated
348 transcripts is a novel mechanism governing the quantitative expression of multiple ion
349 channel types and thus the balance of excitability in the cardiomyocyte.

350

351

352

353

354

355

356 **METHODS**

357

358 **Cell culture, plasmids and transfection**

359 HEK293 cells were cultured under standard conditions (37°C, 5% CO₂) in DMEM medium
360 (Gibco) supplemented with 10% Fetal Bovine Serum (FBS, Gibco). iPSC-CM (iCell[®], Cellular
361 Dynamics International) were plated and cultured following manufacturer's instructions.
362 ShRNA sequences specific for hERG1a 5'-GCGCAGCGGCTTGCTCAACTCCACCTCGG-3'
363 and its control 5'-GCACTACCAGAGCTAACTCAGATAGTACT-3' were provided by Origene
364 into a pGFP-V-RS vector. shRNA specific for hERG1b 5'-CCACAACCACCCTGGCTTCAT-3'
365 and its respective control were purchased from Sigma-Aldrich. For heterologous expression,
366 hERG1a (NM_000238) and hERG1b (NM_172057) sequences were cloned into pcDNA3.1.
367 Transient transfections were performed using 2.5 µl/ml Lipofectamin[™] 2000 (Thermofisher)
368 with 2 µg/ml plasmid. Cells were collected for further analysis 48h after transfection. When
369 needed, a second transfection was performed 24h after the first one with either hERG1a or
370 hERG1b shRNA and the corresponding scrambled shRNA as a control. Cells were then
371 collected for experiments 48h after last transfection.

372

373 **Antibodies**

374 Rabbit anti-hERG1a (#12889 from Cell Signaling, 1:100), rabbit anti-hERG1b (#ALX-215-051
375 from Enzo, 1:100), rabbit anti-pan hERG (#ALX-215-049 from Enzo, 1:3000), rabbit anti
376 Na_v1.5 (#ASC-005 from Alomone or #D9J7S from Cell signaling, 1:500), were used for
377 immunofluorescence, western blot or RNA-IP experiments. Alexa 647 goat anti-rabbit, Alexa
378 488 goat anti-rabbit or Alexa 488 donkey anti-mouse were employed for indirect
379 immunofluorescence or immunoblotting experiments (Thermofisher; 1:1000).

380

381 **RNA isolation and semi-quantitative real-time PCR**

382 RNA isolation and purification were achieved using TriZol reagent (Life Technologies) and
383 RNeasy Mini Kit (Qiagen). RT-qPCR experiments were performed using a TaqMan Gene

384 Expression Assay (Life Technologies) and mRNA expression levels were calculated using
385 the $2^{-\Delta\Delta Ct}$ cycle threshold method. All data were normalized to mRNA level of β -*actin*
386 housekeeping genes. Because iPSC-CMs are subject to inherent biological variability, we
387 used a standardization procedure to normalize the independent biological replicates as
388 previously described⁴¹. Briefly, a log transformation of the normalized relative expression
389 gene level was performed, followed by mean centering and autoscaling of the data set.
390 Results are expressed as average and 95% confidence intervals. Primers were purchased
391 from Invitrogen (*hERG1a*: Hs00165120_m1; *hERG1b*: Hs04234675_m1; *SCN5A*:
392 Hs00165693_m1; *RYR2*: Hs00892883_m1; and β -*actin*: Hs01060665_g1).

393

394 **Immunofluorescence**

395 For immunofluorescence studies, iPSC-CMs were grown on gelatin-coated coverslips, rinsed
396 in PBS three times and fixed in 4% paraformaldehyde for 10 minutes at room temperature.
397 Following fixation, cells were incubated 1h at room temperature with a solution containing
398 0.5% triton 100X for permeabilization and 1% bovine serum albumin along with 10% serums
399 (secondary antibodies species) diluted in PBS to saturate samples and limit nonspecific
400 binding. Cells were then processed for indirect immunofluorescence using a combination of
401 primary and secondary antibodies (see antibodies section above). Cells were washed three
402 times with PBS, incubated with DAPI to counterstain nuclei and mounted with Vectafield
403 mounting medium.

404

405 **Single-molecule fluorescence *in situ* hybridization (smFISH)**

406 FISH was performed using Stellaris® probe sets, which comprised up to 48 oligonucleotides
407 designed to selectively bind in series the targeted transcripts. Probes were designed using
408 the Stellaris™ Probe Designer by LGC Biosearch Technologies with the following
409 parameters: masking level: 5, oligo length: 20 nucleotides, and minimum spacing length: 2
410 nucleotides. Oligonucleotides were labeled with TAMRA or Quasar® 670 dyes for detection of
411 *SCN5A* and *hERG* respectively. 48 oligonucleotides were designed for *SCN5A*, *RyR2* and

412 *GAPDH* and 35 [for](#) the specific N-terminal sequence of *hERG1a*. Sequences for all probes
413 are provided in Supplementary Table 1. FISH was performed on iPSC-CMs according the
414 manufacturer's protocol. Briefly, fixation was performed by adding paraformaldehyde to a
415 final concentration of 4% (32% solution, EM grade; Electron Microscopy Science) followed by
416 a hybridization step for at least 4h at 37°C in a buffer containing a final concentration of 125
417 nM probes and 10% formamide (Stellaris hybridization buffer). Cells were washed for 30 min
418 (Stellaris washing buffer A) before incubation for 30 min at 37°C with DAPI to counterstain
419 the nuclei. A final washing step was performed (Stellaris washing buffer B) and coverglasses
420 were mounted onto the slide with Vectashield mounting medium.

421 Digital images were acquired using a 63X objective on a Leica DMI8 AFC Inverted wide-field
422 fluorescence microscope. Z-sections were acquired at 200 nm intervals. Image pixel size:
423 XY, 106.3 nm. Image post-treatments were performed using ImageJ software (NIH). Briefly,
424 a maximum projection was performed before background subtraction and images were
425 filtered using a Gaussian blur filter to improve the signal/noise ratio and facilitate spot
426 detection. Spot detection and colocalization was performed using the plugin ComDet on
427 ImageJ^{42,43}.

428 FISHQUANT was used as a second method for spot detection and gave similar values.
429 Briefly, background was subtracted using a Laplacian of Gaussian (LoG) and spots were fit
430 to a three-dimensional (3D) Gaussian to determine the coordinates of the mRNA molecules.
431 Intensity and width of the 3D Gaussian were thresholded to exclude non-specific signal^{11,12}.
432 To evaluate the number of mRNA molecules, the total fluorescence intensity of smFISH
433 signals was fitted with the sum of Gaussian functions (see equation below) to determine the
434 mean intensity of a single mRNA.

435

$$y = y_0 + \frac{A}{w\sqrt{\pi}} e^{-2\left(\frac{x-xc}{w}\right)^2}$$

436

437

438 **Statistical analysis of smFISH and IF**

439 For the purpose of our statistical calculations, we assumed that the protein and mRNA
440 signals were circular. The following formulas were used to calculate the expected number of
441 mRNAs (E_m) that would interact based on chance alone for each association criteria:

442

$$E_m = \frac{N_{m1}N_{m2}(2\pi r^2 - I)}{A}$$

443

444 where N_{m1} is the total number of mRNA in one channel, N_{m2} is the total number of mRNA in
445 the second channel, r is the average radius of mRNA spots (in nm), I is the intersection
446 between particles (nm^2), and A is the total area of the region analyzed (in nm^2). As the
447 distance between particles is increased, the number of expected associated mRNAs will
448 increase since more mRNAs will be considered associated. We used criteria with different
449 stringency in the first set of experiments (from 1 pixel to 4 pixels distance between spots) and
450 considered the 2 pixels distance between spots physiologically relevant for triple association
451 analysis and co-knockdown experiments.

452 To test the significance of triple associations between hERG1a mRNA, SCN5A mRNA and
453 hERG1a protein, the following formula was used:

454

$$E_p = \frac{N_p E_m (\pi r^2 - I)}{A}$$

455

456 where N_p is the total number of proteins, E_m is the expected number of mRNA that would
457 interact based on chance alone as calculated above. For each association criteria, the
458 intersection between particles was calculated using the following equation:

459

$$I = 2r^2 \cos^{-1}\left(\frac{d}{2r}\right) - \frac{1}{2}d(\sqrt{4r^2 - d^2})$$

460
461

462 **Correlation analysis**

463 mRNA numbers were plotted against each other from different combinations of smFISH
464 signals as scatter plots. Then Pearson's and Spearman's correlation coefficients were
465 evaluated to assess correlation between considered mRNA species.

466 The following equation was used to calculate Pearson's coefficient R and determine the
467 coefficient of determination R^2 from the mRNA pairs x_i, y_i :

$$R = \frac{Cov(x_i, y_i)}{\sigma_{x_i} - \sigma_{y_i}}$$

468 where $Cov(X_i, Y_i)$ is the covariance of the values and $\sigma_{x_i} - \sigma_{y_i}$ is the difference between the
469 standard deviation of the values. Significance was determine using a F test.

470

471 The Spearman's coefficient ρ was determined on ranked values X_i and Y_i using the following
472 equation:

$$\rho = \frac{Cov(X_i, Y_i)}{\sigma_{X_i} - \sigma_{Y_i}}$$

473 where $Cov(X_i, Y_i)$ is the covariance of the rank values and $\sigma_{X_i} - \sigma_{Y_i}$ is the difference between
474 the standard deviation of the ranked values. Significance was determine using two-tailed
475 probability test.

476

477

478 **RNA-IP (RNA-immunoprecipitation)**

479 Ribonucleoprotein (RNP) complexes were isolated with a RiboCluster Profiler TM RIP-Assay
480 Kit (Medical & Biological Sciences) using protein-specific antibodies and Ab-immobilized A/G
481 agarose beads. After formation of the RNP/beads complex, we used guanidine hydrochloride
482 solution to dissociate beads from RNP complexes. Finally, target RNAs were analyzed using
483 RT-PCR.

484

485 **Electrophysiological measurements**

486 Patch clamp under whole-cell configuration was used to record all ionic currents. I_{Kr} and
487 $I_{Na,late}$ were recorded at physiological temperatures (37°C), while I_{Na} was recorded at room
488 temperature (22°C) using an Axon 200B amplifier and Clampex Software (Molecular
489 Devices). Glass pipettes with a resistance of 2.5 – 5 MΩ measured with physiological
490 solutions (below) were pulled using an automatic P-97 Micropipette Puller system (Sutter
491 Instruments).

492

493 To record steady state and tail I_{Kr} , cells were continuously perfused with an external solution
494 containing (in mM): NaCl 150, KCl 5.4, CaCl₂ 1.8, MgCl₂ 1, Glucose 15, HEPES 15, Na-
495 pyruvate 1, and the pH was adjusted to 7.4 with NaOH. Pipettes were filled with an internal
496 solution containing (in mM): NaCl 5, KCl 150, CaCl₂ 2, EGTA 5, HEPES 10, Mg-ATP 5, and
497 the pH was adjusted to 7.3 with NaOH. The voltage protocol for I_{Kr} was completed at
498 physiological temperature (37°C) and determined as an E-4031 (2μM) sensitive current.
499 Cells were recorded using a holding potential of -50 mV, followed by a pulse at -40 mV to
500 inactivate sodium channels, then 3-second depolarizing steps (from -50 to +30 mV in 10 mV
501 increments) to activate hERG channels and finally to -40 mV for 6 seconds. Steady-state I_{Kr}
502 was measured as the 5 ms average current at the end of the depolarizing steps. Tail currents
503 were measured following the return to -40 mV.

504 To record I_{Na} , cells were perfused with an external solution containing (in mM): NaCl 50,
505 Tetraethylammonium (TEA) methanesulfonate 90, CaCl₂ 2, MgCl₂ 1, Glucose 10, HEPES 10,
506 Na-pyruvate 1, Nifedipine 10 μM, and pH adjusted to 7.4 with TEA-OH. Micropipettes were
507 filled with an internal solution containing (in mM): NaCl 10, CaCl₂ 2, CsCl 135, EGTA 5,
508 HEPES 10, Mg-ATP 5, and pH was adjusted to 7.3 with CsOH.

509 I_{Na} activation was investigated by applying pulses between -140 and +20 mV in 10 mV
510 increments from a holding potential of -120 mV. To measure inactivation of sodium channels,

511 conditioning pulses from -140 to +20 mV in 10 mV increments were applied from a holding
512 potential of -120 mV following by a test pulse to -20 mV.
513 To record $I_{Na,late}$, cells were perfused with an external solution containing (in mM): 140, CsCl
514 5.4, CaCl₂ 1.8, MgCl₂ 2, HEPES 5, Nifedipine 10 μM, and pH was adjusted to 7.3 with NaOH.
515 Pipette were filled with an internal solution containing (in mM): NaCl 5, CsCl 133, Mg-ATP
516 2, TEA 20, EGTA 10, HEPES 5, and pH was adjusted to 7.33 with CsOH. $I_{Na,late}$ was
517 measured by applying an 800 ms single pulse to -30 mV from a holding potential of -120 mV.
518 The mean current was measured at the last 200 ms of the pulse. An external solution
519 containing 30 μM TTX was perfused after the first pulse to determine if the current was due
520 to the activity of sodium channels.
521 To record I_{to} , cells were continuously perfused with an external solution containing (in mM):
522 NaCl 150, KCl 5.4, CaCl₂ 1.8, MgCl₂ 1, Glucose 15, HEPES 15, Na-pyruvate 1, E4031 2,
523 CdCl₂ 0.5 and the pH was adjusted to 7.4 with NaOH. Pipettes were filled with an internal
524 solution containing (in mM): NaCl 5, KCl 150, CaCl₂ 2, EGTA 5, HEPES 10, Mg-ATP 5, and
525 the pH was adjusted to 7.3 with NaOH.
526 Both activation (for I_{Kr} , I_{to} and I_{Na}) and inactivation (for I_{Na}) were fitted to Boltzmann equations
527 (Equations (1) and (2), respectively) and voltage dependence parameters were obtained.

528

$$I(V) = \frac{(V - V_{rev})G_{max}}{1 + e^{\frac{(V-V_{1/2})}{k}}} \quad (1)$$

529

530

$$I(V) = \frac{(I_{min} - I_{max}) + I_{max}}{1 + e^{\frac{(V-V_{max})}{k}}} \quad (2)$$

531

532

533

534 **Acknowledgements**

535 Research reported in this publication was supported by the National Heart, Lung and Blood
536 Institute of the National Institutes of Health R01HL131403. The authors thank Dr. Peter
537 Mohler of the Dorothy Davis Heart and Lung Institute for heart samples and Drs. Barry

538 Ganetzky of the University of Wisconsin-Madison, Andrew Harris of the Rutgers New Jersey
539 Medical School and Drs. Cynthia Czajkowski and Baron Chanda of the University of
540 Wisconsin School of Medicine and Public Health for comments on an earlier version of the
541 manuscript.

542 **Author Contributions**

543 Experiments were conceived and designed by C.A.E, E.R.-P., F.L. and G.A.R. C.A.E. and
544 M.B.J. carried out single molecule FISH experiments. F.L. and J.J.K. conducted RNA-IP and
545 knock-down experiments. E.B.R-P. and D.K.J. performed electrophysiology experiments.
546 C.A.E. and G.A.R. wrote the manuscript and all authors provided critical feedback to the final
547 version.

548

549 **Data Availability**

550 The source data corresponding to Figures 1b, 2b, 2c, 2d, 2e, 3b, 3d, 4b, 4c, 4e, 5b, 5c, 5d,
551 6b, 6c, 6d, 7a, 7b, 7d, 7e, 7g, 7h, 7j, 7k, 8a, 8b, 8d and Supplementary Figures S1, S3a,
552 S3b, S3c, S4a, S4b, S5a, S5b, S6b, S7b, S7c. Raw files images and other data supporting
553 the findings of this study are available upon request.

554

555

556 **Reference list**

- 557 1. Roden, D. M. Predicting drug-induced QT prolongation and torsades de pointes. *J.*
558 *Physiol.* **594**, 2459–2468 (2016).
- 559 2. Sanguinetti, M. C. & Jurkiewicz, N. K. Two components of cardiac delayed rectifier
560 K⁺ current. Differential sensitivity to block by class III antiarrhythmic agents. *J. Gen.*
561 *Physiol.* **96**, 195–215 (1990).
- 562 3. Sanguinetti, M. C., Jiang, C., Curran, M. E. & Keating, M. T. A mechanistic link
563 between an inherited and an acquired cardiac arrhythmia: HERG encodes the IKr potassium
564 channel. *Cell* **81**, 299–307 (1995).
- 565 4. Trudeau, M. C., Warmke, J. W., Ganetzky, B. & Robertson, G. A. HERG, a human
566 inward rectifier in the voltage-gated potassium channel family. *Science* **269**, 92–95 (1995).
- 567 5. Sale, H. *et al.* Physiological properties of hERG 1a/1b heteromeric currents and a
568 hERG 1b-specific mutation associated with Long-QT syndrome. *Circ. Res.* **103**, e81-95
569 (2008).
- 570 6. Jones, E. M. C., Roti, E. C. R., Wang, J., Delfosse, S. A. & Robertson, G. A. Cardiac

- 571 IKr Channels Minimally Comprise hERG 1a and 1b Subunits. *J. Biol. Chem.* **279**, 44690–
572 44694 (2004).
- 573 7. Phartiyal, P., Jones, E. M. C. & Robertson, G. A. Heteromeric Assembly of Human
574 Ether-à-go-go-related Gene (hERG) 1a/1b Channels Occurs Cotranslationally via N-terminal
575 Interactions. *J. Biol. Chem.* **282**, 9874–9882 (2007).
- 576 8. McNally, B. A., Pendon, Z. D. & Trudeau, M. C. hERG1a and hERG1b potassium
577 channel subunits directly interact and preferentially form heteromeric channels. *J. Biol. Chem.*
578 **292**, 21548–21557 (2017).
- 579 9. Liu, F., Jones, D. K., de Lange, W. J. & Robertson, G. A. Cotranslational association
580 of mRNA encoding subunits of heteromeric ion channels. *Proc. Natl. Acad. Sci. U. S. A.* **113**,
581 4859–4864 (2016).
- 582 10. Jones, D. K. *et al.* hERG 1b is critical for human cardiac repolarization. *Proc. Natl.*
583 *Acad. Sci.* **111**, 18073–18077 (2014).
- 584 11. Raj, A., van den Bogaard, P., Rifkin, S. A., van Oudenaarden, A. & Tyagi, S. Imaging
585 individual mRNA molecules using multiple singly labeled probes. *Nat. Methods* **5**, 877–879
586 (2008).
- 587 12. Femino, A. M., Fay, F. S., Fogarty, K. & Singer, R. H. Visualization of Single RNA
588 Transcripts in Situ. *Science* **280**, 585–590 (1998).
- 589 13. Azzam, M. E. & Algranati, I. D. Mechanism of Puromycin Action: Fate of Ribosomes
590 after Release of Nascent Protein Chains from Polysomes. *Proc. Natl. Acad. Sci.* **70**, 3866–
591 3869 (1973).
- 592 14. Glynn, P. *et al.* Voltage-Gated Sodium Channel Phosphorylation at Ser571 Regulates
593 Late Current, Arrhythmia, and Cardiac Function In Vivo. *Circulation* **132**, 567–577 (2015).
- 594 15. Banyasz, T., Horvath, B., Jian, Z., Izu, L. T. & Chen-Izu, Y. Sequential dissection of
595 multiple ionic currents in single cardiac myocytes under action potential-clamp. *J. Mol. Cell.*
596 *Cardiol.* **50**, 578–581 (2011).
- 597 16. Sun, X. & Wang, H.-S. Role of the transient outward current (I_{to}) in shaping canine
598 ventricular action potential – a dynamic clamp study. *J. Physiol.* **564**, 411–419 (2005).
- 599 17. Tu, L. & Deutsch, C. Evidence for dimerization of dimers in K⁺ channel assembly.
600 *Biophys. J.* **76**, 2004–2017 (1999).
- 601 18. Robinson, J. M. & Deutsch, C. Coupled tertiary folding and oligomerization of the T1
602 domain of Kv channels. *Neuron* **45**, 223–232 (2005).
- 603 19. Rook, M. B. *et al.* Human SCN5A gene mutations alter cardiac sodium channel
604 kinetics and are associated with the Brugada syndrome. *Cardiovasc. Res.* **44**, 507–517 (1999).
- 605 20. Bezzina, C. *et al.* A single Na⁽⁺⁾ channel mutation causing both long-QT and Brugada
606 syndromes. *Circ. Res.* **85**, 1206–1213 (1999).
- 607 21. Bennett, P. B., Yazawa, K., Makita, N. & George, A. L. Molecular mechanism for an
608 inherited cardiac arrhythmia. *Nature* **376**, 683 (1995).
- 609 22. Clancy, C. E., Tateyama, M., Liu, H., Wehrens, X. H. T. & Kass, R. S. Non-
610 equilibrium gating in cardiac Na⁺ channels: an original mechanism of arrhythmia. *Circulation*
611 **107**, 2233–2237 (2003).
- 612 23. Schulz, D. J., Goillard, J.-M. & Marder, E. E. Quantitative expression profiling of
613 identified neurons reveals cell-specific constraints on highly variable levels of gene
614 expression. *Proc. Natl. Acad. Sci. U. S. A.* **104**, 13187–13191 (2007).
- 615 24. Schulz, D. J., Goillard, J.-M. & Marder, E. Variable channel expression in identified
616 single and electrically coupled neurons in different animals. *Nat. Neurosci.* **9**, 356–362
617 (2006).
- 618 25. Dar, R. D. *et al.* Transcriptional burst frequency and burst size are equally modulated
619 across the human genome. *Proc. Natl. Acad. Sci. U. S. A.* **109**, 17454–17459 (2012).
- 620 26. Brown, V. *et al.* Microarray identification of FMRP-associated brain mRNAs and

- 621 altered mRNA translational profiles in fragile X syndrome. *Cell* **107**, 477–487 (2001).
- 622 27. Keene, J. D. & Tenenbaum, S. A. Eukaryotic mRNPs May Represent
623 Posttranscriptional Operons. *Mol. Cell* **9**, 1161–1167 (2002).
- 624 28. Gerber, A. P., Herschlag, D. & Brown, P. O. Extensive Association of Functionally
625 and Cytotopically Related mRNAs with Puf Family RNA-Binding Proteins in Yeast. *PLoS*
626 *Biol.* **2**, (2004).
- 627 29. García-Rodríguez, L. J., Gay, A. C. & Pon, L. A. Puf3p, a Pumilio family RNA
628 binding protein, localizes to mitochondria and regulates mitochondrial biogenesis and motility
629 in budding yeast. *J. Cell Biol.* **176**, 197–207 (2007).
- 630 30. Ule, J. *et al.* CLIP Identifies Nova-Regulated RNA Networks in the Brain. *Science*
631 **302**, 1212–1215 (2003).
- 632 31. Duncan, C. D. S. & Mata, J. Widespread Cotranslational Formation of Protein
633 Complexes. *PLoS Genet.* **7**, (2011).
- 634 32. Duncan, C. D. & Mata, J. Cotranslational protein-RNA associations predict protein-
635 protein interactions. *BMC Genomics* **15**, 298 (2014).
- 636 33. Cosker, K. E., Fenstermacher, S. J., Pazyra-Murphy, M. F., Elliott, H. L. & Segal, R.
637 A. The RNA-binding protein SFPQ orchestrates an RNA regulon to promote axon viability.
638 *Nat. Neurosci.* **19**, 690–696 (2016).
- 639 34. Petersen, C. P., Bordeleau, M.-E., Pelletier, J. & Sharp, P. A. Short RNAs repress
640 translation after initiation in mammalian cells. *Mol. Cell* **21**, 533–542 (2006).
- 641 35. Maroney, P. A., Yu, Y., Fisher, J. & Nilsen, T. W. Evidence that microRNAs are
642 associated with translating messenger RNAs in human cells. *Nat. Struct. Mol. Biol.* **13**, 1102–
643 1107 (2006).
- 644 36. Yang, T. *et al.* Blocking Scn10a channels in heart reduces late sodium current and is
645 antiarrhythmic. *Circ. Res.* **111**, 322–332 (2012).
- 646 37. Macri, V. *et al.* Common Coding Variants in SCN10A Are Associated With the
647 Nav1.8 Late Current and Cardiac Conduction. *Circ. Genomic Precis. Med.* **11**, e001663
648 (2018).
- 649 38. Isom, L. L., De Jongh, K. S. & Catterall, W. A. Auxiliary subunits of voltage-gated
650 ion channels. *Neuron* **12**, 1183–1194 (1994).
- 651 39. Milstein, M. L. *et al.* Dynamic reciprocity of sodium and potassium channel
652 expression in a macromolecular complex controls cardiac excitability and arrhythmia. *Proc.*
653 *Natl. Acad. Sci. U. S. A.* **109**, E2134–2143 (2012).
- 654 40. Matamoros, M. *et al.* Nav1.5 N-terminal domain binding to α 1-syntrophin increases
655 membrane density of human Kir2.1, Kir2.2 and Nav1.5 channels. *Cardiovasc. Res.* **110**, 279–
656 290 (2016).
- 657 41. Willems, E., Leyns, L. & Vandesompele, J. Standardization of real-time PCR gene
658 expression data from independent biological replicates. *Anal. Biochem.* **379**, 127–129 (2008).
- 659 42. Chang, L., Shav-Tal, Y., Trcek, T., Singer, R. H. & Goldman, R. D. Assembling an
660 intermediate filament network by dynamic cotranslation. *J. Cell Biol.* **172**, 747–758 (2006).
- 661 43. Hoffman, D. B., Pearson, C. G., Yen, T. J., Howell, B. J. & Salmon, E. D.
662 Microtubule-dependent Changes in Assembly of Microtubule Motor Proteins and Mitotic
663 Spindle Checkpoint Proteins at PtK1 Kinetochores. *Mol. Biol. Cell* **12**, 1995–2009 (2001).
- 664

665

666

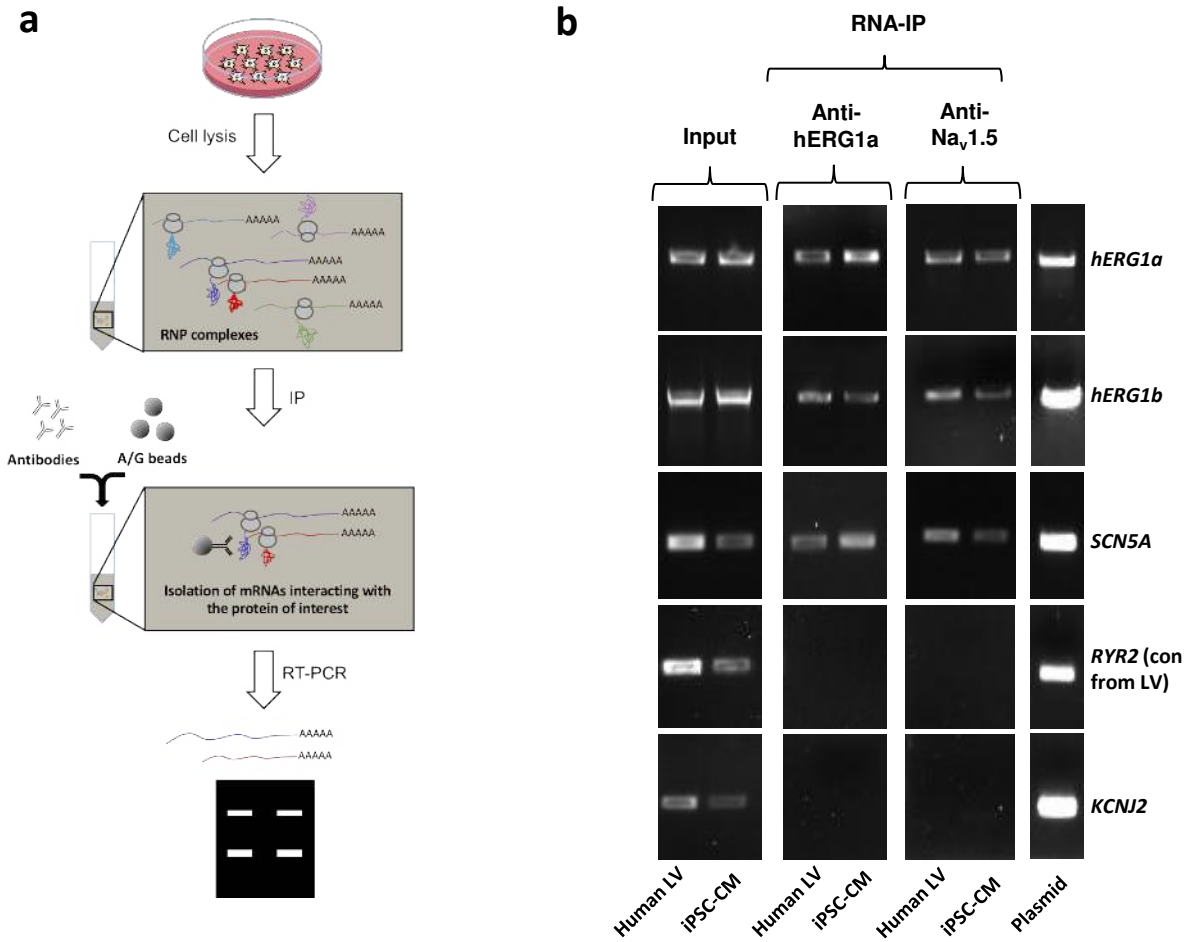


Figure 1: Complex of ion channel transcripts with nascent proteins. **a**, Scheme of the RNA-IP protocol in which channel-specific antibodies are used to pull down nascent proteins and associated transcripts. RNP: ribonucleoprotein. **b**, Lanes 1 and 2, RT-PCR products from input lysate of human left ventricle (LV), and iPSC-CM. Lanes 3-16 shows the corresponding RNA-IP's using an anti-hERG1a or anti-Na_v1.5 antibodies; Lane 7 shows the control (+) and represents signal amplified from purified plasmid template. Similar results were obtained in at least 3 independent experiments. (N=5 for anti-hERG1a and N=3 for anti-Na_v1.5 using human LV and iPSC-CMs).

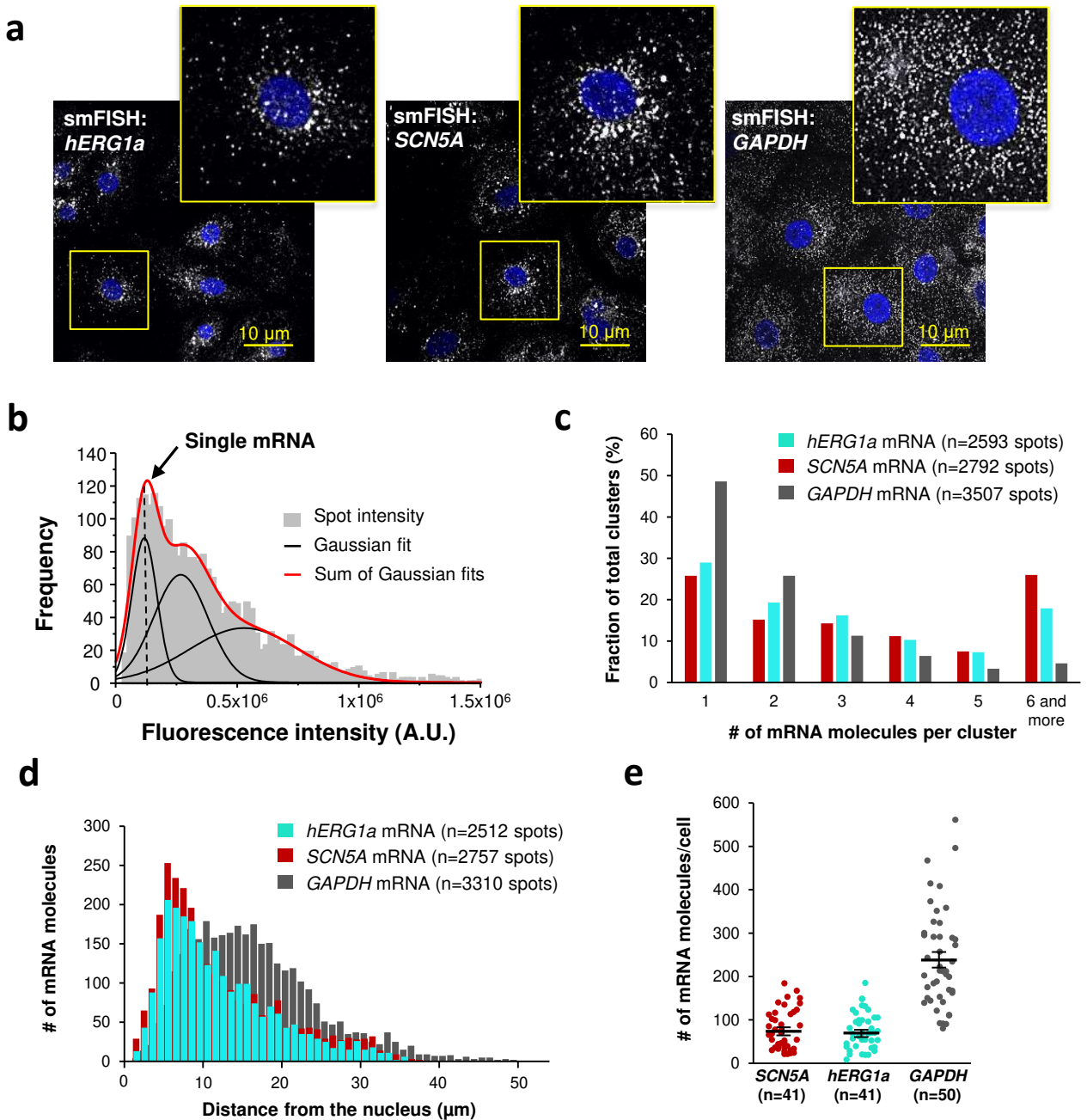


Figure 2: Quantitative description of single *hERG1a* and *SCN5A* transcripts and their distribution in iPSC-CMs. **a**, Representative confocal images and enlargement (outlined in yellow) of iPSC-CMs subjected to the smFISH protocol. **b**, By fitting the intensity histogram of smFISH signals (n=2611 spots) to the sum of Gaussian functions (red line), the typical intensity corresponding to a single mRNA molecule (vertical dashed line) was extracted. **c**, The distribution of the number of mRNA molecules associated in clusters for each transcript evaluated by smFISH. **d**, Histogram showing the cytoplasmic distribution of mRNA signals with distance from the nucleus. **e**, The number of mRNAs detected per cell was plotted for *SCN5A*, *hERG1a* and *GAPDH* (lines represent mean \pm SE).

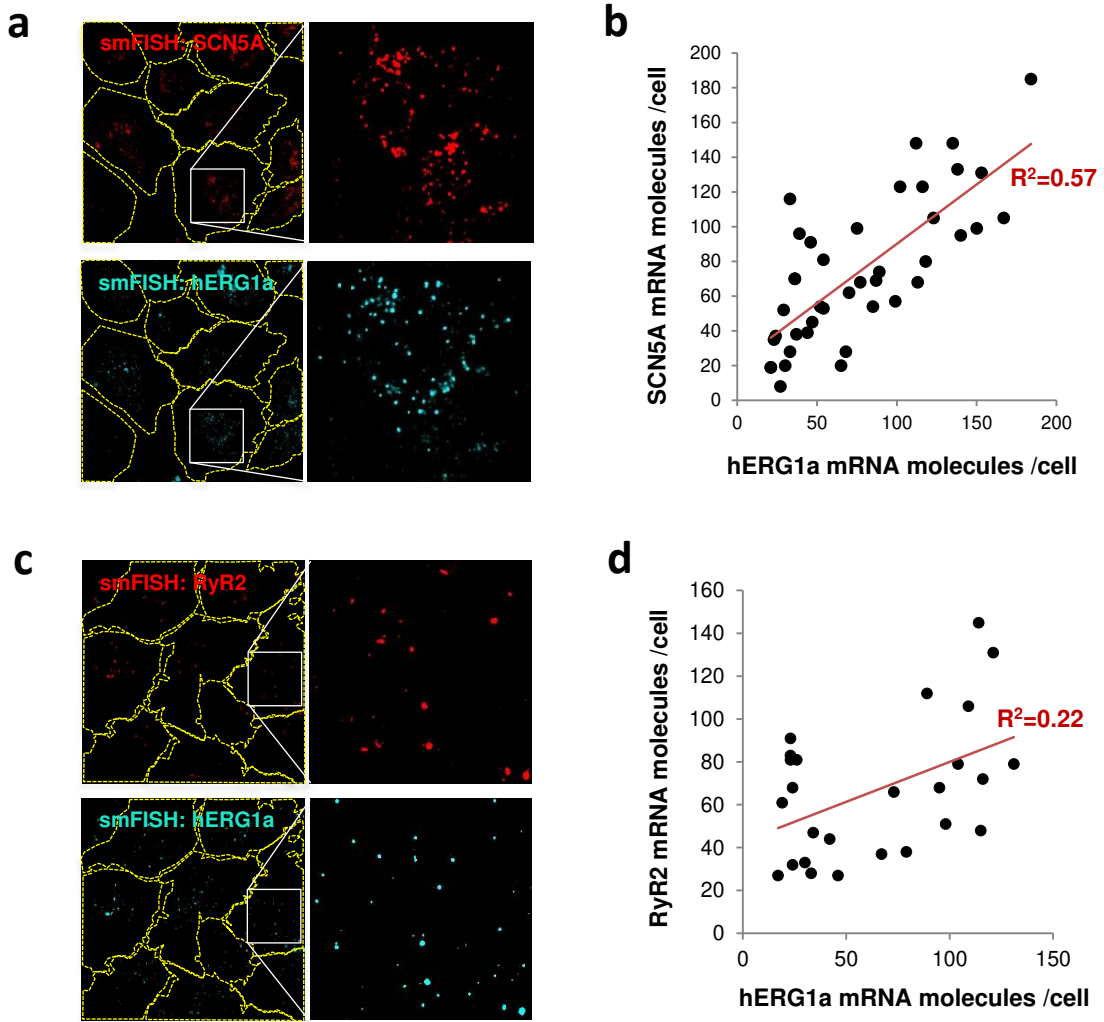


Figure 3: *hERG1a* and *SCN5A* transcript expression levels correlate. **a**, Representative confocal images and enlargements of double smFISH experiments for *SCN5A* (red) and *hERG1a* (cyan) mRNAs. **b**, The number of mRNA molecules detected per cell in double smFISH experiments were plotted for *SCN5A* and *hERG1a* and the coefficient of determination R^2 was determined from the Pearson's correlation coefficient R ($n=41$ cells; $N=2$). **c**, Representative confocal images and enlargements of double smFISH experiments for *RyR2* (red) and *hERG1a* (cyan) mRNAs. **d**, The number of *hERG1a* mRNA was plotted against the number of *RyR2* mRNAs per cells and showed a low correlation in their expression ($n=26$ cells; $N=2$).

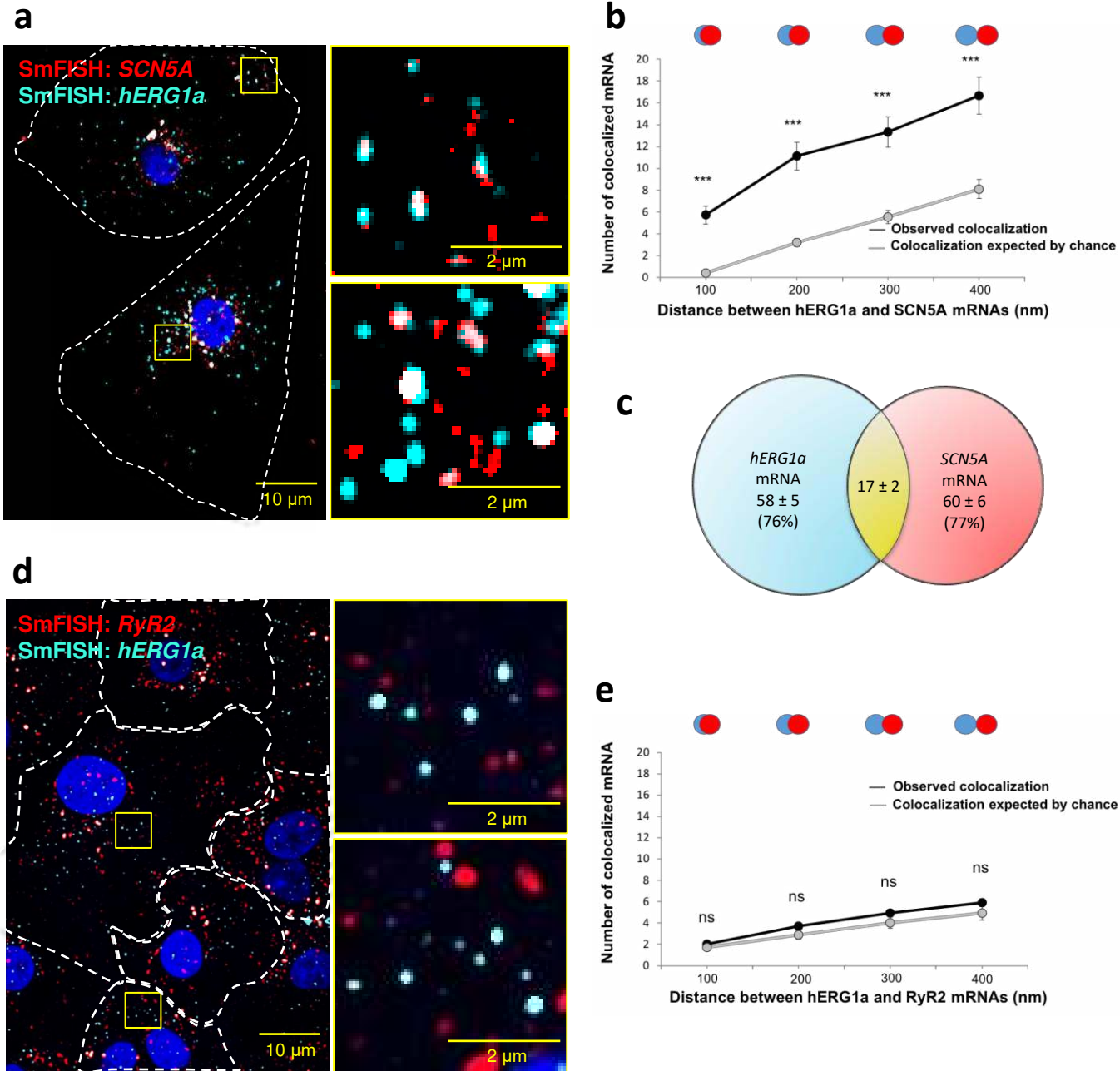


Figure 4: *hERG1a* and *SCN5a* transcript colocalization. **a**, Representative confocal images and enlargement (outlined in yellow) of iPSC-CMs subjected to smFISH showing the colocalization of *hERG1a* and *SCN5a* mRNAs. **b**, Comparison of the average number of associated *hERG1a* and *SCN5a* mRNAs particles observed vs. expected by chance using different overlap criteria illustrated (mean \pm SE; $n=41$ cells; $N=2$). **c**, Diagram illustrating that the association of *hERG1a* and *SCN5a* mRNAs account for 24% and 23% of their total population respectively. **d**, Representative confocal images of smFISH for *hERG1a* and *RyR2* transcripts. **e**, Comparison of the average number of associated *hERG1a* and *RyR2* mRNAs particles observed vs. expected by chance using different overlap criteria (mean \pm SE; $n=26$ cells; $N=2$).

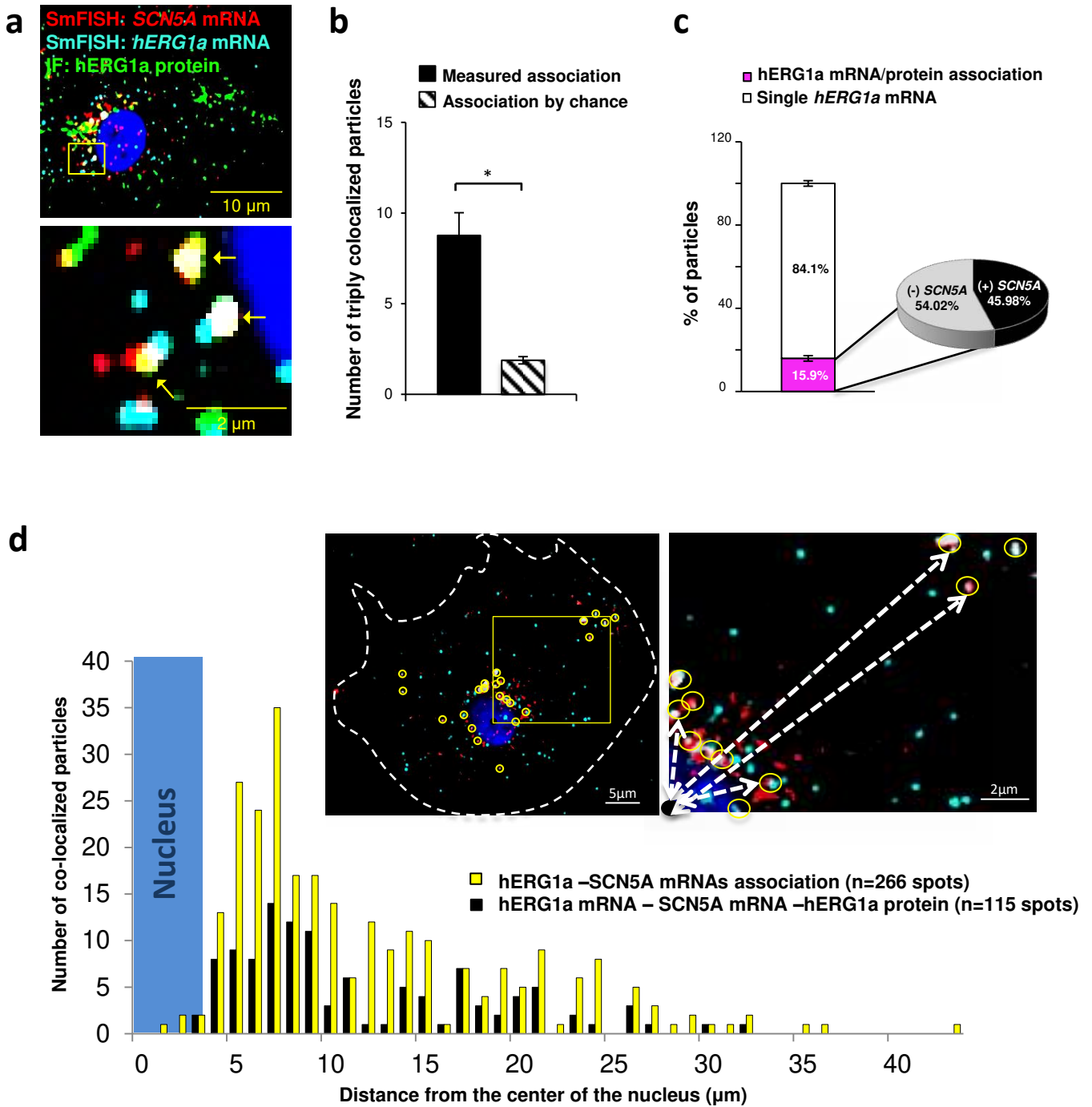


Figure 5: Cotranslational association of *hERG1a* protein and *hERG1a* and *SCN5A* mRNAs. a, Representative confocal images and enlargement of iPSC-CMs subjected to immunofluorescence (IF) combined with smFISH protocol. Arrows indicate triply colocalized particles. **b,** The average number of particles comprising *hERG1a* and *SCN5A* mRNAs and *hERG1a* protein per cell compared to the expected number based on chance using a maximum distance of 2 pixels between center of mass (minimum 50% overlap; mean \pm SE; n=13 cells, N=2). **c,** Histogram showing that 16% of *hERG1a* mRNA associate with *hERG1a* protein (actively translated population); of that percentage, 46% also interact with *SCN5A* transcripts.(mean \pm SE; n=13 cells; N=2) **d,** Histogram showing the distribution of colocalized mRNA spots through the cytoplasm and from the nucleus revealing that RNP complexes are mostly localized within 10 μm from the nucleus. In the top right corner, representative examples of colocalized spots (yellow circles) and analysis of distance from the nucleus (white dashed arrows).

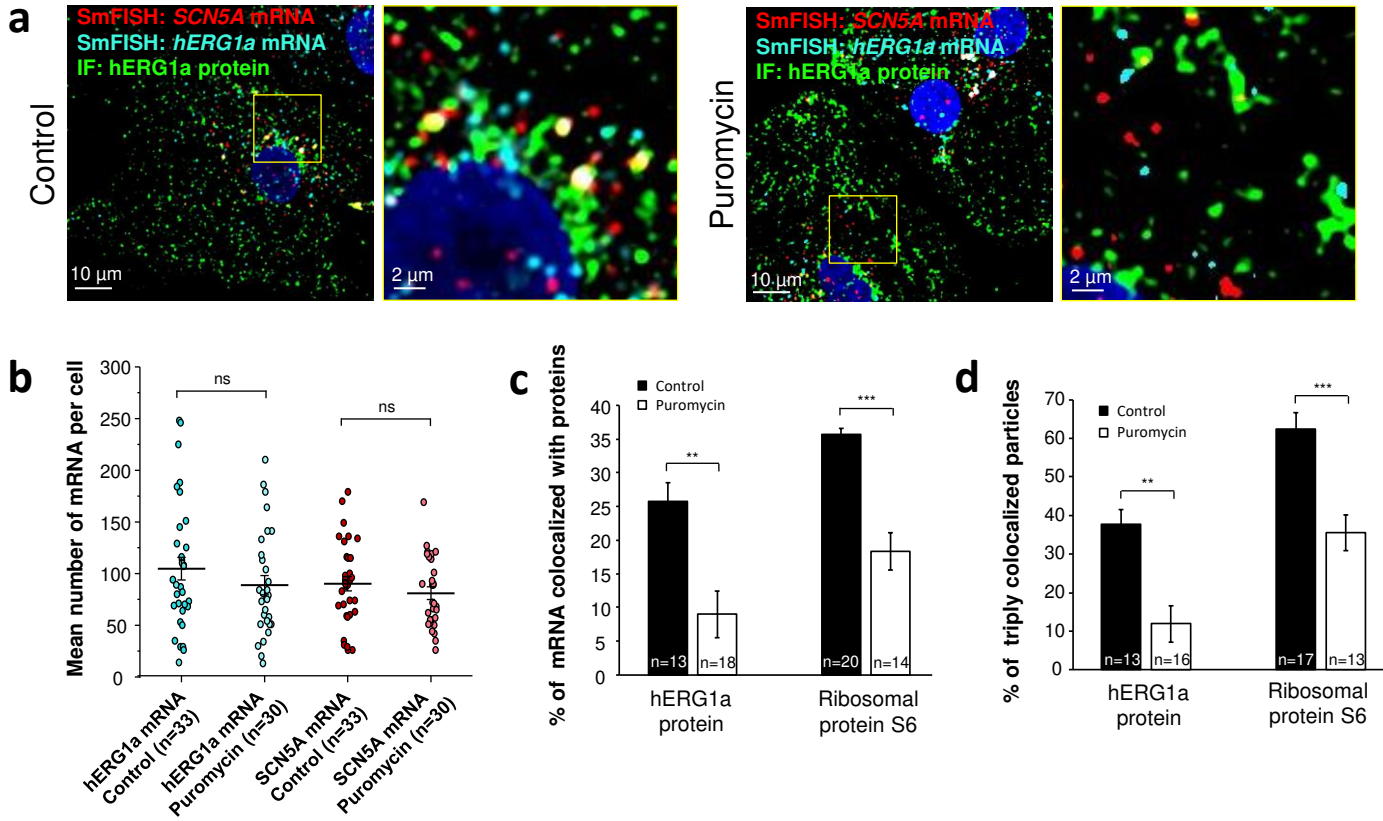


Figure 6: Distribution and association of *hERG1a* and *SCN5A* transcripts under puromycin treatment in iPSC-CMs. **a**, Representative confocal images and enlargement (outlined in yellow) of iPSC-CMs subjected to immunofluorescence combined with smFISH for control cells (left panel) or cells treated with 100 μ M puromycin for 15 min (right panel). **b**, The number of mRNAs detected per cell was plotted for *SCN5A* and *hERG1a* in the presence of puromycin and compared to control cells (lines represent mean \pm SE). **c**, Histogram showing the reduction of association between *hERG1a* mRNA and hERG1a protein after puromycin treatment compared to non-treated cells (mean \pm SE). **d**, Histogram showing that the % of triply colocalized particles (hERG1a protein or the ribosomal subunit S6 associated with both *hERG1a* and *SCN5A* mRNAs) is decreased upon puromycin treatment (mean \pm SE).

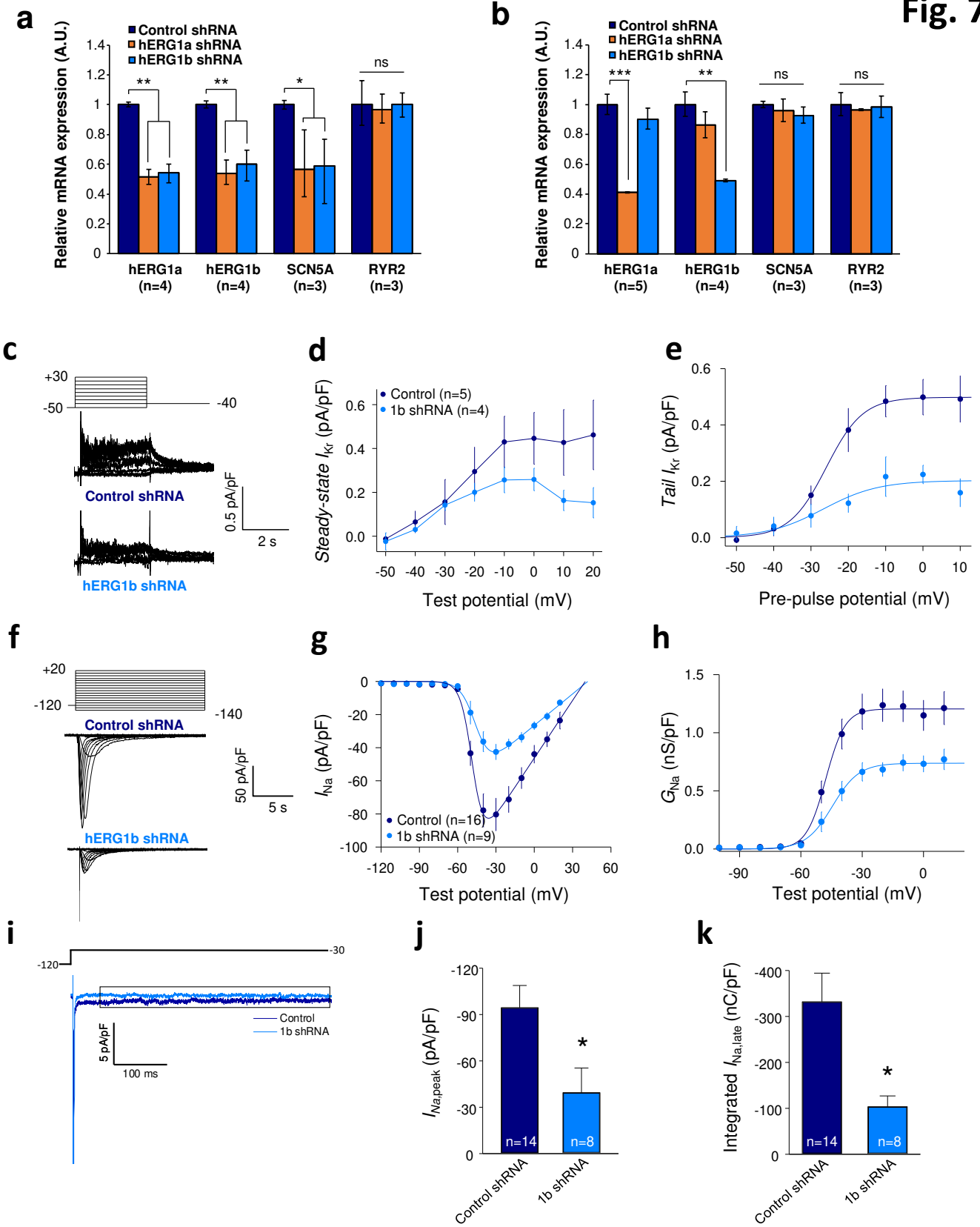


Figure 7: Co-knockdown of I_{Kr} and I_{Na} by hERG transcript-specific shRNA. **a**, Effects of *hERG1a* or *hERG1b* silencing on channel mRNA expression levels detected by RT-qPCR (mean \pm 95% CI) in iPSC-CMs. A non-targeting shRNA (scrambled shRNA) is used as a control. **b**, Effects of specific *hERG1a* or *hERG1b* silencing on ion channel mRNAs expressed alone in HEK293 cells. **c**, Representative family of traces show I_{Kr} in presence of control (upper) or hERG1b shRNA (lower). **d**, Summary of steady-state current density vs. test potential shows effect of hERG1b shRNA (mean \pm SE). **e**, Effects of 1b shRNA on peak tail current vs. pre-pulse potential (mean \pm SE). **f**, Representative family of traces recorded from iPSC-CMs showing effects of hERG1b-specific shRNA compared to control shRNA on peak I_{Na} . **g**, Summary current-voltage plot of peak I_{Na} vs. test potential (mean \pm SE). **h**, Summary conductance (G)-voltage plot based on data from *g* (mean \pm SE). **i**, Late sodium current representative trace in control and 1b shRNA-transfected cells, measured by applying a single pulse protocol of 800 ms. **j**, Summary statistics of peak I_{Na} showed a decrease upon transfection with hERG1b shRNA (mean \pm SE). **k**, Late I_{Na} measured as the integral from 50 to 800 ms from the beginning of the pulse showed a decrease upon transfection with hERG1b shRNA (mean \pm SE).

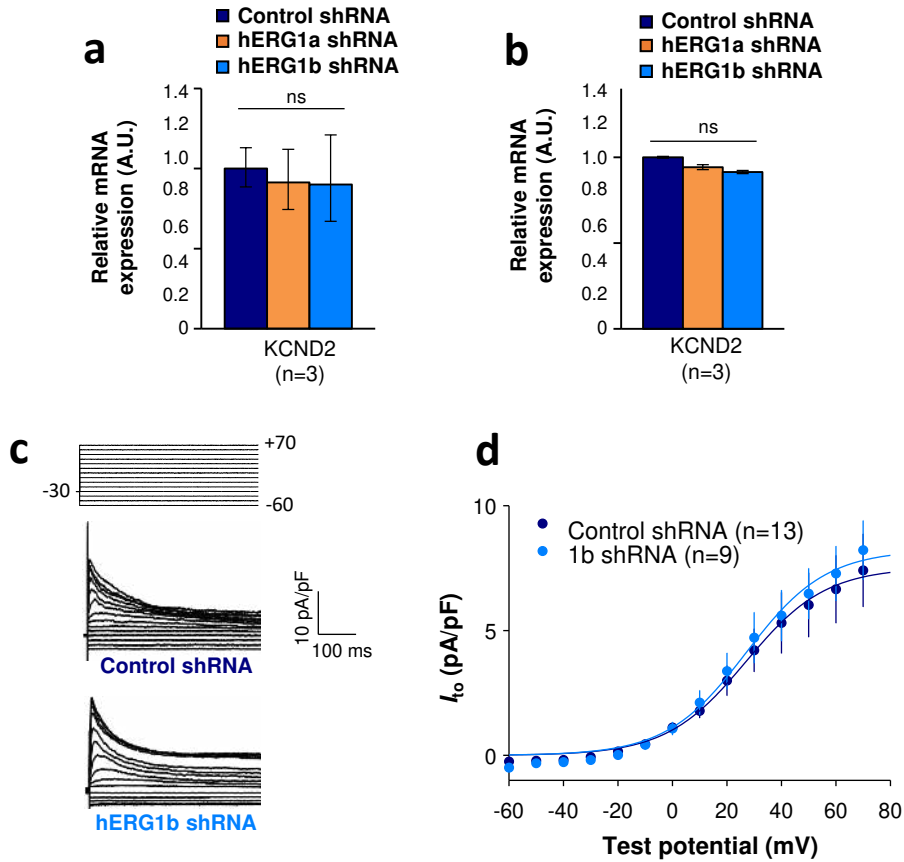


Figure 8: Effects of hERG1b silencing on I_{to} and $K_{V4.2}$ channels in iPSC-CMs. **a**, Effects of *hERG1a* or *hERG1b* silencing on $K_{V4.2}$ channel mRNA expression levels detected by RT-qPCR (mean \pm 95%CI) in iPSC-CMs. A non-targeting shRNA (scrambled shRNA) is used as a control. **b**, Effects of specific *hERG1a* or *hERG1b* silencing on $K_{V4.2}$ channel mRNAs expressed alone in HEK293 cells. **c**, Representative family of traces show I_{to} in presence of control (upper) or hERG1b shRNA (lower). **d**, Summary of steady-state current density vs. test potential shows effect of hERG1b shRNA (mean \pm SE).

Supplementary

Table S1

hERG1a probes	SCN5A probes	RyR2 probes
caagactggactgcgggc	cccgaggtaataggaagttt	tccatntttccacatcaact
agcactaggcttcgggtg	tagagatctggcagcttttt	acatccaatntttccttgga
caggaaggtgttctgcgg	agtcttttgggtgctataga	tgtagatcccattctcac
acttgcggatgatgggtg	gaagatggcttgcctttat	catgtcgggatctcgacaaa
aacttacggctctgcccc	ggactgaggacatacaaggc	caaggcccttataaatcta
ccgagcgttggcagatgat	gtgtactcgacatacttggg	gaagtagccaatgagatcct
agatgacggcgagttct	gaccagagactcaaagggtg	tctgttctgttcttcat
cagaagccgtcgttgacag	ccgaaggaaagtgaacgcgt	agtcgaggagccagaaaaat
cgagtagccgcacagctc	aatcacactaaagtccagcc	acatccagaaccttgtgatt
gcagggtcgtgcatcac	attcagttgtgatgccatg	tggcaaacacagagtgagca
cgtgcaggaagtgcaggg	tcgctaaggctgagacattg	tcacagatgagatgctggtt
cagtgcctgcgcgatctg	ccaggcaaaggaatcgaagc	atggttcacaagacgtgtct
gatttccactttgcgctc	caggcggaaagagtgaagaa	gatgaaggccatcaaatcca
cccatcttccggtagaa	tcagtaaacgggtccatgac	ttggtgagcttacagtacga
ccaccagacataggaagc	tgtgtgagtagcatgcaca	aggttgcattaattcgga
ctcgttcttcacggggcac	tctcgaattcacttctcat	agttcttcttcttcttact
aacatgatgacagccca	gggcaatgatctgaaggtc	acttgcagctggtaattct
ccacctcgaattgagga	tggaagtagtaggggtc	tatgtgcattttctgccaac
accatgtccttccatc	gatgacgatgatgtctcga	ggaacaaggcgaggatttct
gtggttgggtcatgagc	ccgatgatctttagatgtgt	cacggaagattcgaacctt
cttcaggcggaaaggtctt	gaacacgatgatggctagca	gtgtgaacatcatggtgtgt
ctgtcacttctccaggg	agtagttcttccaagagc	ctgacatccttccaagatt
tgccacgtggttgcctat	aggttgccaatgaccataac	atggtaatatcctctgttgt
gtcggggttgggctgtg	atgaatgtctgaaccagct	cagtgttctgttctgagaa
cttctcgggagcgcgtc	ctactgctgagtaggatcatg	ttctcggcataatctttg
catggcctcagatgctgc	ctaggtagatgctctcgaag	ggcttcttcttctaagcaa
tcgcagtggtgcatgg	caagcagaacctttaggtc	tactgtgacgttgcataca
gtggagttgagcaagccg	atctccagcacgaagacata	agtcaaacctgtgtcatal
cacgaggtcggagtccga	agtacttctgaagccgtag	tggcaatgaatgtgagcagc
tgctaattggtcggtagc	aatcgtgacagagctctcag	ggactttagcttctgcaaaa
ttgaggtgatttgggga	cgaggaggacgttcatgatg	gagagaggcatcaccattctt
gccccttgaggtccacaaa	tgttcacgatggttagttc	ttcttctgctcacttctgaa
gcgaagccaagaaggggt	agttcaaggactcacactgg	ttcgagacacatctacctc
gatctcacggtcactggt	ccacgttgcataaagttgact	gggacaatgtactctgttgtt
ctcctttatcttaggtgc	gctgcatacataatgtccat	gcttcaaaaactgggggagg
	tcctctgtcatgaagatgct	acacactgggctcaatcaac
	catggcattgtagtacttct	ttgatctgttctttaggtgg
	aatatgaagccctgttactt	agacgcctctaattgttaa
	catcatggtcaccatattca	agtactctcaactggtttt
	cagcttgacaatacactcgc	gggtcttcaatgacagactc
	ttggtgaagtagtagtggcg	ctccgaatgagcaatctcac
	tggagaggatgacaaccag	atggacctaatctgatggc
	aagagcgtcggggagaagaa	tgaacctcaatccatagac
	catcatgagggcaagagca	ctgtgcaaaggtaccgattg
	acatgacgaggaagagcagc	agagaggagcacatcttgtt
	ccatgccaagatggagtag	gaacagcccttagaagctct
	cccacttgacataagcgaag	aaactctatggaatccgc
	taggagatcttggatgggtt	ttctgagtaagtctgcatc

Table S1: List of probes used in smFISH experiments. The probes were designed using Stellaris® probe Designer software with the following parameters: 18 to 20 nucleotides oligo length, a masking level of 5, a minimum spacing length of 2 nucleotides and a maximum number of probes of 48. Due to the length of the N-terminal specific sequence for *hERG1a* mRNA, the number of probes used to detect *hERG1a* is limited to 35.





		 400 nm Touching	 300 nm 20% overlap	 200 nm 45% overlap	 100 nm 67% overlap	
hERG1a/SCN5A (n=41 cells)	Expected by chance Measured P value	8.10 ± 0.87 16.68 ± 1,70 1.57E-9 (***)	5.56 ± 0.61 13.34 ± 1.38 4.71E-9 (***)	3.20 ± 0,34 11.12 ± 1.28 3.49E-10 (***)	0.40 ± 0.04 5.73 ± 0.82 4.51E-8 (***)	Significance after Bonferroni's correction: * P≤0.00125; ** P≤0.000122; *** P≤0.0000244
hERG1a/RyR2 (n=26 cells)	Expected by chance Measured P value	4.92 ± 0.66 5.92 ± 0.36 0.16 (ns)	4.03 ± 0.54 4.96 ± 0.30 0.16 (ns)	2.88 ± 0.39 3.69 ± 0.26 0.14 (ns)	1.74 ± 0,23 2.04 ± 0,24 0.38 (ns)	Significance after Bonferroni's correction: * P≤0.00197; ** P≤0.000193; ***P≤0.0000385
hERG1a/GAPDH (n=13 cells)	Expected by chance Measured P value	14.87 ± 2.65 13.54 ± 1.68 0.53 (ns)	7.47 ± 1.33 8.46 ± 1.15 0.20 (ns)	5,48 ± 1,23 5,24 ± 0,72 0.19 (ns)	0.54 ± 0.10 0.92 ± 0.15 0.24 (ns)	Significance with Bonferroni correction: * P≤0.0039; ** P≤0.000386; ***P≤0.000077
SCN5A/GAPDH (n=28 cells)	Expected by chance Measured P value	17.31 ± 1.71 15.92 ± 1.64 0.16 (ns)	12.73 ± 1.25 9.92 ± 1.04 0.002 (ns)	6.82 ± 0.67 5.32 ± 0.60 0.0006 (*)	0.92 ± 0.09 1.62 ± 0.28 0.012 (ns)	Significance after Bonferroni's correction: * P≤0.0013; ** P≤0.000186; *** P≤0.0000275

Table S2: Summary of colocalization analysis performed in iPSC-CMs for different association criteria. Comparison of the average number of mRNAs particles observed to be associated and the expected number based on chance alone using centroid positions and different association criteria (from touching to 67% overlap). The significance is tested with a paired t-test Bonferroni's correction. The number of *hERG1a* and *SCN5A* mRNAs observed to be associated is significantly above that expected by chance alone for all association criteria tested while no significant differences are observed for *hERG1a/RyR2*, *hERG1a/GAPDH* and *SCN5A/GAPDH* associations.

		hERG1a/SCN5A (41 cells)	hERG1a/RyR2 (26 cells)	hERG1a/GAPDH (13 cells)	SCN5A/GAPDH (28 cells)
Pearson's test	Correlation coefficient R	0.7546	0.4654	0.4197	0.4808
	Coefficient of determination R ²	0.56943	0.2166	0.1761	0.2315
	P value	0.00001 (***)	0.01658 (*)	0.153373 (ns)	0.0096 (*)
	Slope of linear regression line	0.6844	0.3732	0.2662	1.4651
	Significance after Bonferroni correction	* P<0.038 ** P<0.0076 *** P<0.00076	* P<0.024 ** P<0.0049 *** P<0.00049	* P<0.023 ** P<0.0046 *** P<0.00046	* P<0.025 ** P<0.005 *** P<0.0005
Spearman's test	Correlation coefficient ρ	0.7449	0.3224	0.4890	0.3692
	P value	0 (***)	0.1084 (ns)	0.08991 (*)	0.05315 (ns)
	Significance after Bonferroni correction	* P<0.019 ** P<0.0039 *** P<0.00039	* P<0.0055 ** P<0.0011 *** P<0.00011	* P<0.013 ** P<0.0027 *** P<0.00027	* P<0.0061 ** P<0.0012 *** P<0.00012

Table S3: Summary of correlation analysis performed in iPSC-CMs. The linear correlation between the different combination of mRNAs was evaluated using the Pearson correlation coefficient. Because the Pearson coefficient is highly sensitive to outliers and only assess linear correlation, the Spearman's correlation coefficient was also calculated. Both tests revealed a significant correlation between hERG1a and SCN5A mRNAs and no significant correlation for *hERG1a/RyR2*, *hERG1a/GAPDH* and *SCN5A/GAPDH* pairs. Levels of significance were adjusted with a Bonferroni correction taking into account correlation coefficients and either linear correlation or non-linear correlation for Pearson's and Spearman's test respectively.

Table S4 and S5

Condition	G_{\max} (nS/pF) or I_{\max} (pA/pF)	$V_{1/2}$ (mV)	k (mV)	V_{rev} (mV)	n
Activation					
Control	1.22 ± 0.1	-45.9 ± 1.1	-4.7 ± 0.4	36.5 ± 3.0	16
1b shRNA	0.73 ± 0.1	-45.7 ± 1.6	-4.8 ± 0.5	31.7 ± 3.2	9
Inactivation					
Control	-54.1 ± 7.7	-89.8 ± 1.3	7.2 ± 0.3		16
1b shRNA	-33.2 ± 9.7	-88.6 ± 1.9	6.8 ± 0.5		9

Table S4: Voltage dependence of activation and inactivation parameters for the sodium channels in cells transfected with a control shRNA or a hERG1b specific shRNA. Parameters were obtained after fitting to a Boltzmann equation activation and inactivation data.

Condition	$I_{\max \text{ peak-tail}}$ (pA/pF)	$V_{1/2}$ (mV)	k (mV)	n
Control	0.50 ± 0.01	-26.0 ± 0.5	5.6 ± 0.5	5
1b shRNA	0.21 ± 0.03	-23.1 ± 4.5	7.1 ± 5.3	4

Table S5: Voltage dependence of activation of hERG channels in cells transfected with a control shRNA or a hERG1b specific shRNA. Parameters were obtained by fitting the experimental data of the I-V curve of the peak tail I_{Kr} to a Boltzmann equation.

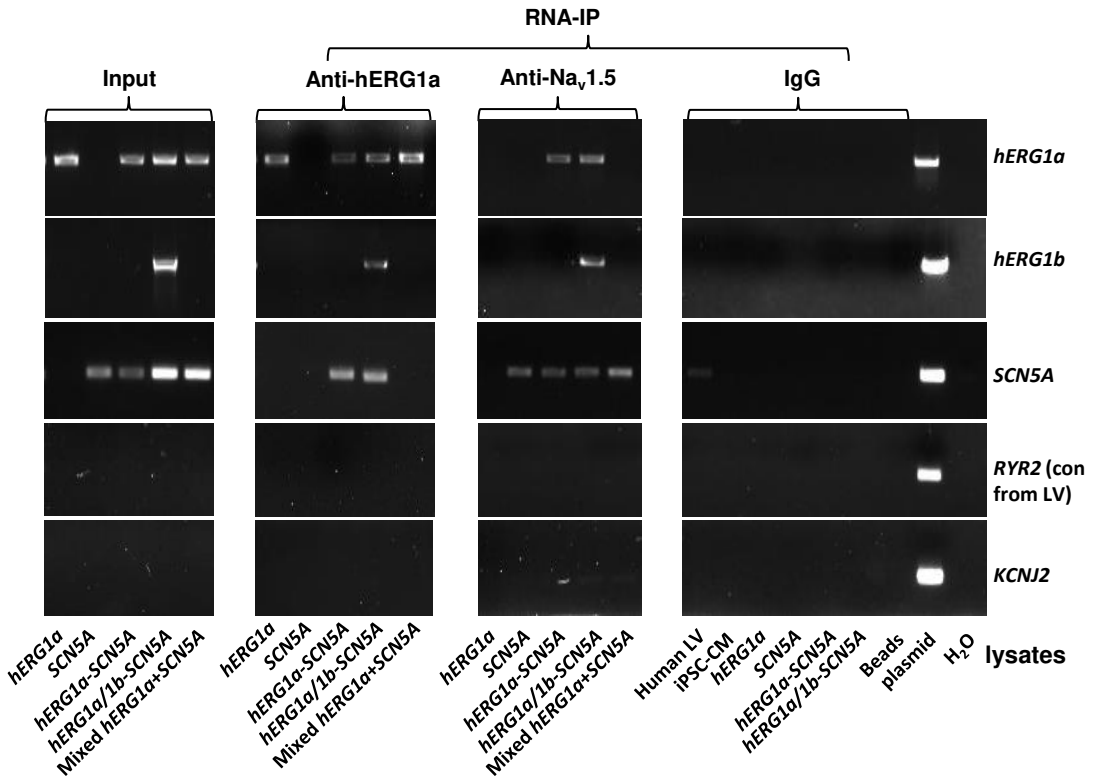


Figure S1: Complete RNA-IP from Figure 1. Lanes 1-6, RT-PCR products from input lysate of human left ventricle (LV), iPSC-CM, and HEK293 cells expressing: *hERG1a*; *SCN5A*; *hERG1a* plus *SCN5A*; and *hERG1a* plus *hERG1b* and *SCN5a*. Lane 7 shows RT-PCR product from lysates independently expressing *hERG1a* and *SCN5A*, mixed. Lanes 8-14 shows the corresponding RNA-IP's using an anti- *hERG1a* antibody, followed by a bead-only control and H₂O control. The next group shows the corresponding RNA-IP's using the anti-Nav1.5 antibody, followed by a group of IgG controls. H₂O and beads lanes show absence of template contamination; control (+) represents signal amplified from purified plasmid template.

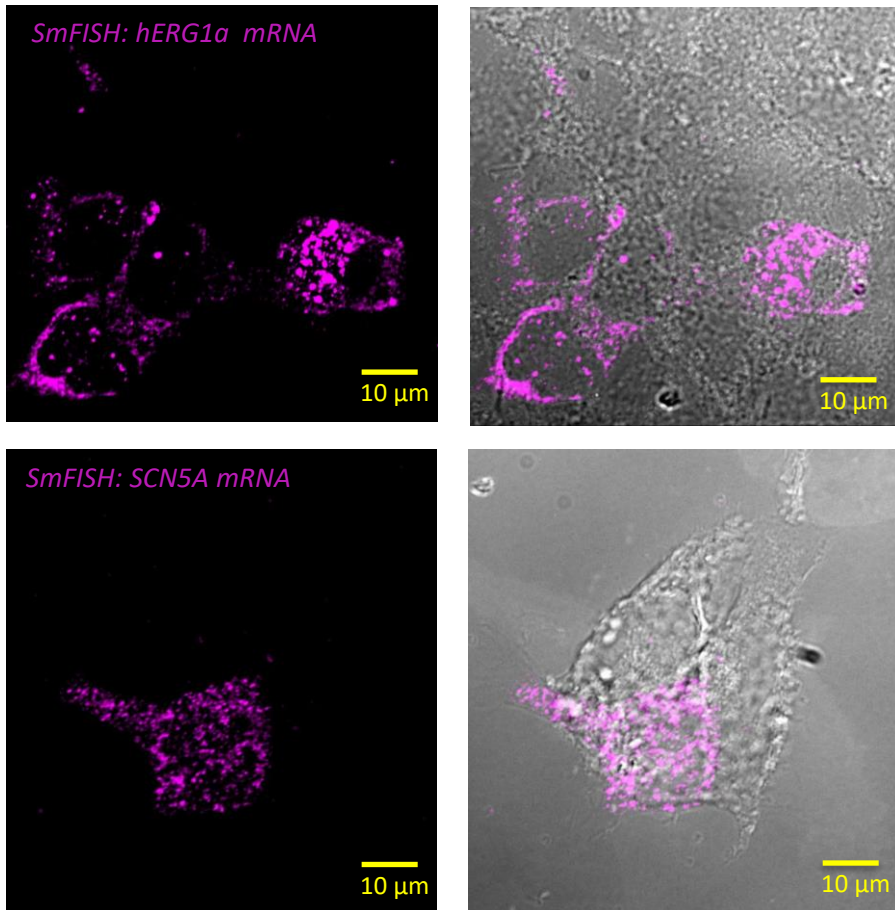
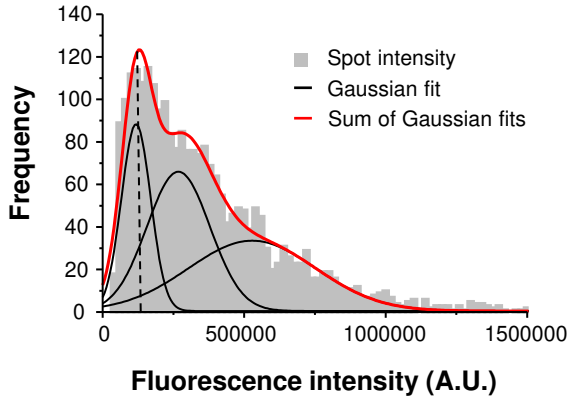


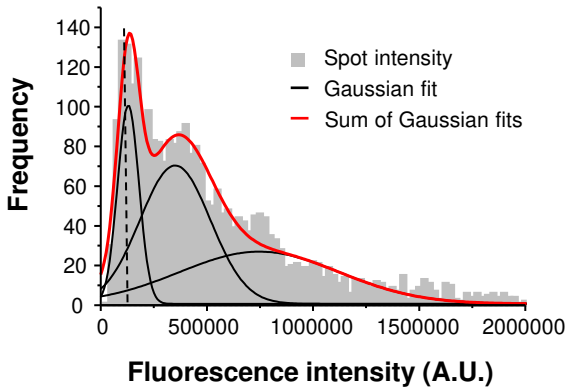
Figure S2: Specificity of the probes used in smFISH experiments. Representative images of smFISH for either *hERG1a* (top panel) or *SCN5A* (bottom panel) mRNAs performed in HEK293 cells transiently transfected with *hERG1a* or *SCN5A*. Only the cells expressing *hERG1a* or *SCN5A* showed a positive signal for smFISH revealing the specificity of the probes used in smFISH experiments.

a *hERG1a* mRNA



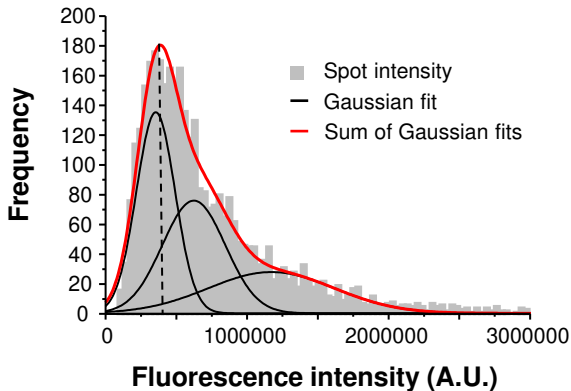
Model	Gauss		
Equation	$y=y_0 + (A/(w*\sqrt{\pi/2}))*\exp(-2*((x-xc)/w)^2)$		
Plot	Peak1	Peak2	Peak3
y0	0.49 ± 0.21	0.49 ± 0.21	0.49 ± 0.21
xc	117984.83 ± 2256.31	267703.93 ± 14735.19	527984.86 ± 76758.94
w	103169.32 ± 7458.84	222635.33 ± 40129.29	450302.22 ± 78120.74
A	1.14E7 ± 2.16E6	1.83E7 ± 6.81E6	1.87E7 ± 5.78E6

b *SCN5A* mRNA



Model	Gauss		
Equation	$y=y_0 + (A/(w*\sqrt{\pi/2}))*\exp(-2*((x-xc)/w)^2)$		
Plot	Peak1	Peak2	Peak3
y0	0.71 ± 0.25	0.71 ± 0.25	0.71 ± 0.25
xc	129681.69 ± 1775.62	350694.45 ± 10021.78	746868.44 ± 133741.99
w	100467.91 ± 5381.31	332189.87 ± 38494	754612.46 ± 142927.70
A	1.26E7 ± 1.15E6	2.90E7 ± 7.35E6	2.48E7 ± 7.91E6

c *GAPDH* mRNA



Model	Gauss		
Equation	$y=y_0 + (A/(w*\sqrt{\pi/2}))*\exp(-2*((x-xc)/w)^2)$		
Plot	Peak1	Peak2	Peak3
y0	0.35 ± 0.31	0.35 ± 0.31	0.35 ± 0.31
xc	354447.18 ± 11207.17	623535.81 ± 117199.66	1.17E6 ± 238744.98
w	274182.43 ± 29650.81	444264.04 ± 165298.03	893413.86 ± 242256.38
A	4.64E7 ± 2.18E7	4.21E7 ± 3.35E7	3.10E7 ± 1.51E7

Figure S3: Single mRNA intensity determination. The distribution of total fluorescence intensity of smFISH signals for *hERG1a* (2611 spots; **a**), *SCN5A* (2815 spots; **b**), and *GAPDH* (3507 spots; **c**). By fitting the histogram to the sum of Gaussian functions (red line), the typical intensity corresponding to a single mRNA molecule (vertical dashed line) was extracted.

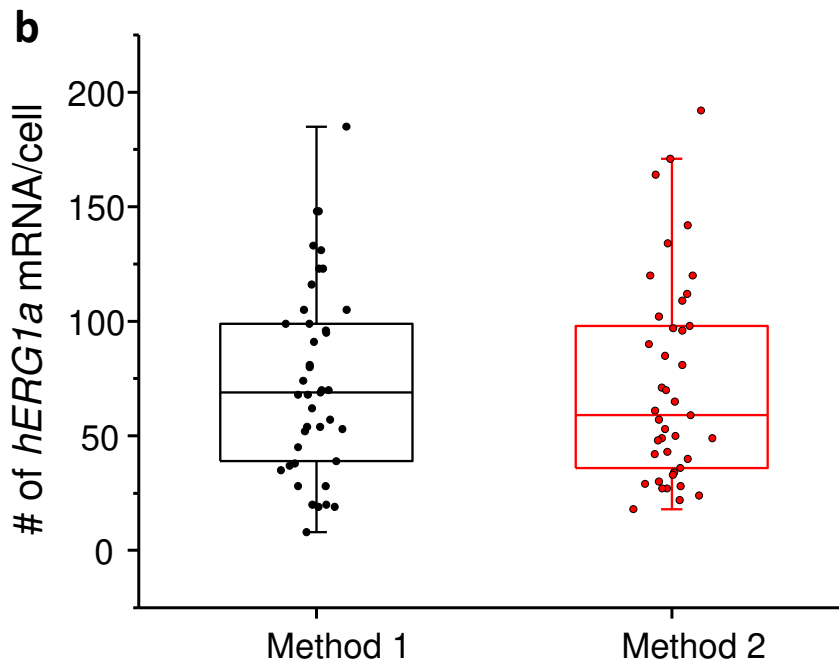
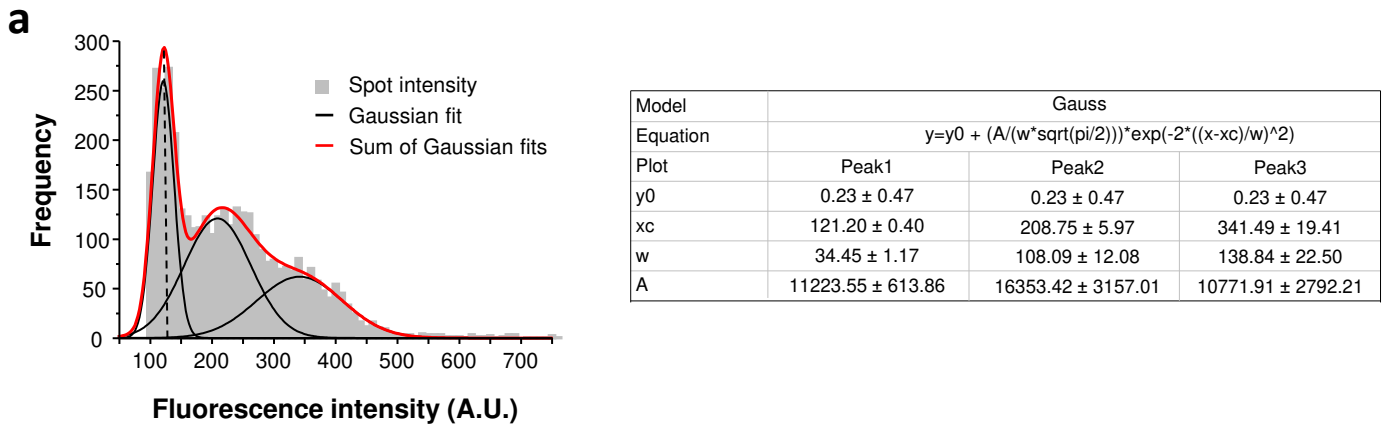


Figure S4: Quantification of mRNA expression using two different methods. **a**, The distribution of total fluorescence intensity of smFISH signals for *hERG1a* (2892 spots) obtained using FISHQUANT software for analysis. By fitting the histogram to the sum of Gaussian functions (red line), the typical intensity corresponding to a single mRNA molecule (vertical dashed line) was extracted. **b**, Comparison of the number of mRNA molecules detected per cells for *hERG1a* using 2 different methods of analysis (Method 1: manual using ImageJ; Method 2: Semi-automatic using FISHQUANT).

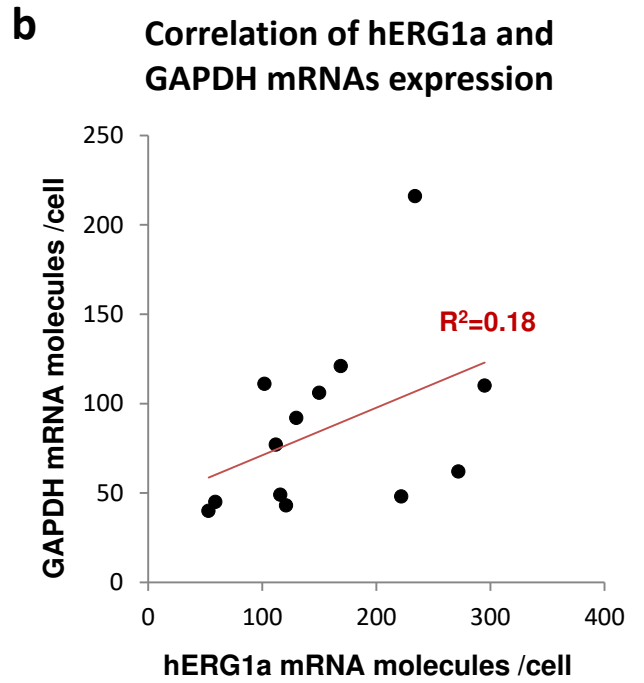
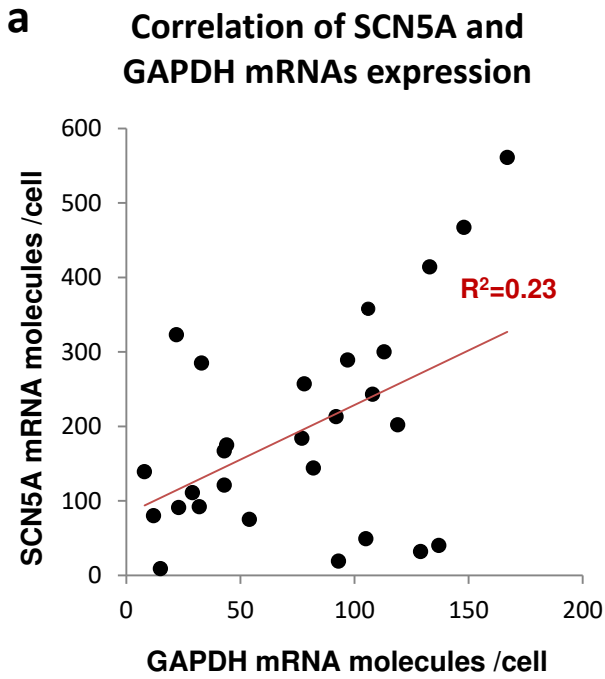


Figure S5: Correlation of mRNA expressions. The number of mRNA molecules detected per cells in double smFISH experiments were plotted for *SCN5A* and *GAPDH* (28 cells, **a**), and *hERG1a* and *GAPDH* (13 cells, **b**). The Pearson's correlation coefficient (R^2) were calculated for each pairs of mRNAs.

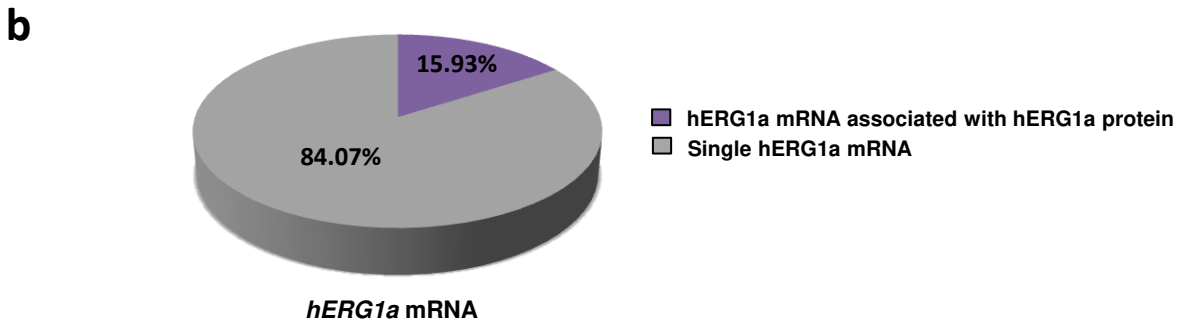
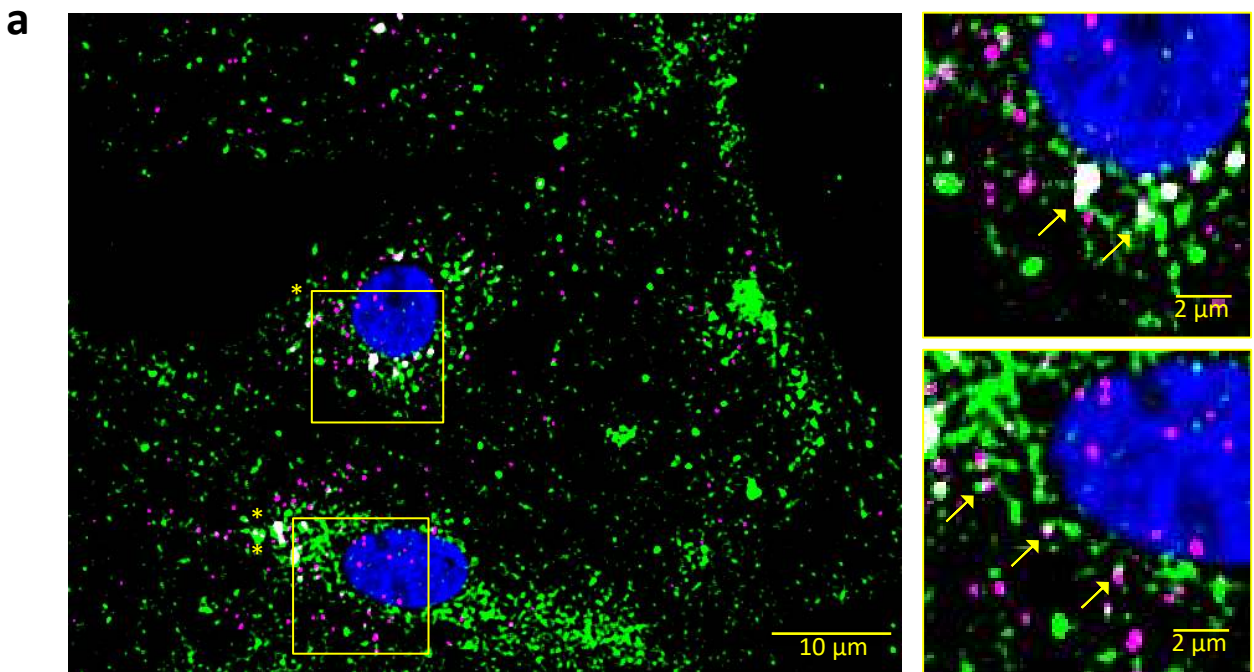


Figure S6: hERG1a mRNA protein interaction. **a**, Representative confocal images and enlargement (outlined in yellow) of iPSC-CMs subjected to Immunofluorescence combined to smFISH protocol showing the colocalization (yellow arrows) of *hERG1a* mRNA (magenta) and hERG1a protein (green). **b**, Pie chart showing the percentage of *hERG1a* mRNA population interacting with hERG1a protein revealing that 16% of *hERG1a* mRNA were actively translated at the moment of fixation.

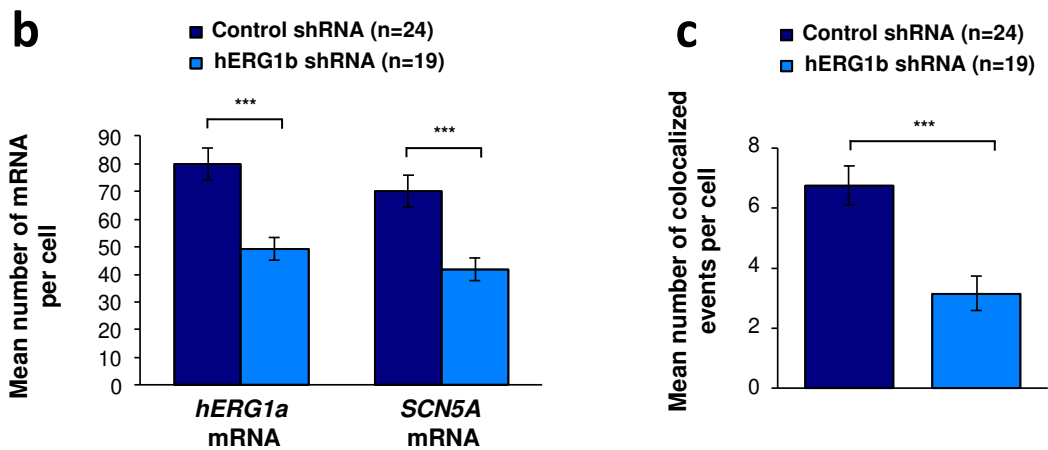
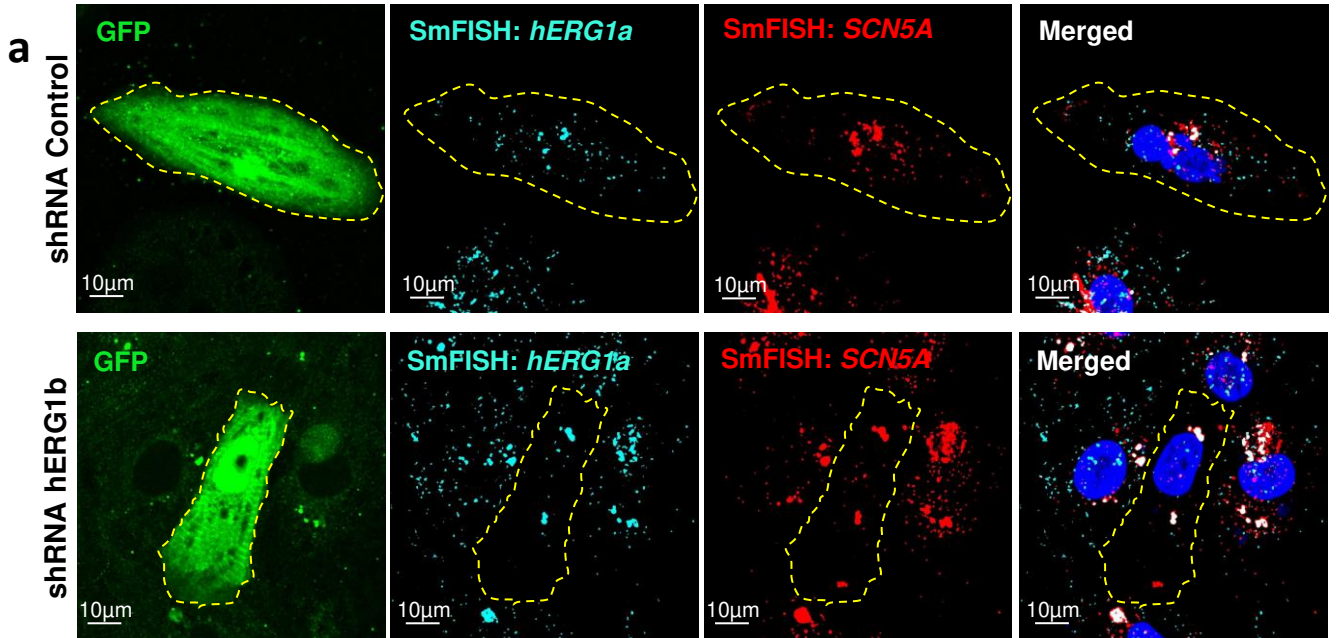


Figure S7: Co-knockdown of *hERG* and *SCN5A* mRNAs by *hERG* transcript-specific shRNA. a, Representative confocal images of smFISH for *hERG1a* and *SCN5A* transcripts in iPSC-CMs transfected with either a control or *hERG1b* shRNA. **b,** Histogram of the average number of transcripts detected per cell for *hERG1a* or *SCN5A* transcripts in presence of *hERG1b* shRNA compared to a scrambled shRNA (mean \pm SE). **c,** Histogram of the mean number of *hERG1a* transcript colocalized with *SCN5A* transcript in cells silenced for *hERG1b* compared with control (mean \pm SE).